AN INVESTIGATION OF A METHOD FOR DETERMINING THE PRESSURE DISTRIBUTION ON AN ACCELERATING FLAT PLATE AT AN ANGLE OF ATTACK AT HYPERSONIC OR SUPERSONIC VELOCITIES

A THESIS

Presented to the

Faculty of the Graduate Division

by

Clarence William Hannon

In Partial Fulfillment

of the Requirements for the Degree

Master of Science in Aeronautical Engineering

Georgia Institute of Technology

June, 1962

5Δ
12R

AN INVESTIGATION OF A METHOD

FOR DETERMINING THE PRESSURE DISTRIBUTION

ON AN ACCELERATING FLAT PLATE

AT AN ANGLE OF ATTACK

AT

HYPERSONIC OR SUPERSONIC VELOCITIES

Approved:

James E. Hubbartt

Frank M. White, Jr.

M. R. Carstens

Date Approved by Chairman: May 26, 1962

"In presenting the dissertation as a partial fulfillment of the requirements for an advanced degree from the Georgia Institute of Technology, I agree that the Library of the Institution shall make it available for inspection and circulation in accordance with its regulations governing materials of this type. I agree that permission to copy from, or to publish from, this dissertation may be granted by the professor under whose direction it was written, or, in his absence, by the dean of the Graduate Division when such copying or publication is solely for scholarly purposes and does not involve potential financial gain. It is understood that any copying from, or publication of, this dissertation which involves potential financial gain will not be allowed without written permission.

ACKNOWLEDGMENTS

The author expresses his sincere appreciation to Professor James E. Hubbartt for his invaluable suggestions and guidance throughout all phases of this investigation. Gratitude is also extended to Dr. Frank M. White, Jr., for the suggestion of the topic and to Drs. White and M. R. Carstens for their review and comments on the material contained herein.

TABLE OF CONTENTS

	Page
ACKNOWLEDGMENTS	ii
LIST OF FIGURES	iv
LIST OF SYMBOLS	v
SUMMARY	vii
CHAPTER	
I. INTRODUCTION	1
II. THE PHYSICAL PROBLEM AND WAVE EQUATIONS	4
III. HYPERSONIC CASE	10
Part A. Numerical-Graphical Solution	
Part B. Analytic Solution	
IV. SUPERSONIC CASE	35
V. CONCLUSIONS	49
APPENDIX	51
Figures	
BIBLIOGRAPHY	71

LIST OF FIGURES

Figure		Page
1.	The Physical Problem	56
2.	Numerical Integration of Wave Equations in ϵ-τ Plane For a Sudden Decrease in Piston Velocity	57
3.	Relation Between x, y, D_{s_o}, β and θ for Flat Plate	58
4.	ϵ-τ Plane for Step Deceleration of Flat Plate From M = 6.0 to M = 5.0	59
5.	Pressure versus τ for Step Deceleration of Flat Plate from M = 6.0 to M = 5.0	60
6.	Pressure versus Time and Distance for Step Deceleration of Flat Plate from M = 6.0 to M = 5.0	61
7.	ϵ-τ Plane for Development of Analytic Solution	62
8.	Pressure versus M and $(\beta - \theta)$ for No Reflections	63
9.	Pressure versus M and $(\beta - \theta)$ for One Reflection	64
10.	Pressure versus M and $(\beta - \theta)$ for Two Reflections	65
11.	Pressure versus M and $(\beta - \theta)$ for Two Reflections with Modified Piston Theory	66
12.	Relation Between Piston, Shock and Disturbance Wave for Determination of Time Lapse	67
13.	Time for One Reflection Versus Mach Number	68
14.	Illustration of Steady State Nature of Problem	69
15.	Illustration of Supersonic Case	70

LIST OF SYMBOLS

A	Non-dimensional ratio a/a_1
a	Speed of sound, feet per second
C	Speed of propagation of wave or shock
C_p	Pressure coefficient
c_p	Specific heat at constant pressure
D	Distance from flat plate surface to shock wave
f	Frequency of oscillation
g	Acceleration due to gravity
M	Mach number
P	Riemann variable, $\frac{2}{\gamma-1} A + U$
p	Pressure
Q	Riemann variable, $\frac{2}{\gamma-1} A - U$
R	Gas constant
S	Non-dimensional entropy, $\frac{s}{\gamma R}$
s	Entropy, shock
t	Time
U	Non-dimensional ratio, u/a_1
u	Flow velocity
w	Wave
x	Distance measured perpendicular to flat plate surface
y	Distance measured along flat plate surface
z	Distance measured along shock wave
β	Angle between horizontal and shock wave
γ	Ratio of specific heats

δ Angle between shock wave and reflected wave

η Time for one wave reflection

θ Angle between horizontal and flat plate surface

ϵ Non-dimensional distance

ρ Density of air

τ Non-dimensional time

ϕ Angle between two shock waves

ψ Angle between entropy interface and reflected wave

SUBSCRIPTS

o Initial conditions

p Piston

s Shock wave

w Wave

1 Conditions in free stream

SUMMARY

The purpose of this paper is to investigate the use of piston theory and the theory of characteristics, considering the entropy gradient across the attached shock, for the determination of the pressure distribution along an accelerating flat plate at an angle of attack. Both the hypersonic and supersonic velocity regimes are considered.

The general wave equations which describe the motion of plane pressure disturbance waves in the area between the flat plate and the shock wave are developed. The flat plate is considered as an accelerating piston which causes pressure disturbance waves to propagate to and be reflected from the shock wave and resulting entropy interfaces.

In the hypersonic regime, the angle between the shock wave and flat plate is assumed to be small so that the change in flow velocity is essentially perpendicular to the flat plate surface and the propagating and reflecting waves are essentially parallel to each other.

A numerical-graphical solution to the problem for the hypersonic regime is obtained by the numerical integration of the wave equations in the x-t plane. Sample calculations are presented for the case of an instantaneous deceleration of a flat plate at an angle of attack of 10° from a Mach number of 6.0 to a Mach number of 5.0.

An analytic solution to the problem is then developed and the pressure change for zero, one and two reflections, divided by the steady state pressure change is plotted versus the Mach number and the

angle between the flat plate and shock wave, $(\beta-\theta)$. An expression for the time required for the reflections to take place is also developed. As a result of this work, an extension of Lighthill's work on the oscillating airfoil, is presented.

It is shown in the hypersonic case that:

(1) The hypersonic solution is accurate to within one per cent for values of Mach number greater than 5.6,

(2) a modified piston theory could be used which would give accuracies within one per cent down to a Mach number of 4.0,

(3) the first reflection of the disturbance waves from the shock wave accounts for the major correction of the pressure back toward steady state value,

(4) the second reflection also contributes a non-negligible correction, but higher order reflections may be neglected,

(5) the reflection time for a disturbance wave is so short that for normal accelerations, the problem may be considered as essentially a steady state problem, and

(6) the hypersonic theory developed is directly applicable to the case of an oscillating flat plate.

In the supersonic case, the piston theory is shown to result in extreme errors. The theory of characteristics is developed for a complete step-by-step solution to the supersonic case. Equations are developed for the most difficult case, that of matching conditions at the shock wave. The disturbance wave network existing between the flat plate and the shock wave is discussed and a step-by-step solution for this wave network and the resulting pressure distribution outlined.

The solution of a complete problem for the supersonic case is recommended for further investigation.

CHAPTER I

INTRODUCTION

The high rate of acceleration and deceleration associated with the firing of today's missiles and rockets has made necessary a better understanding and a more accurate determination of the change in pressure distribution which occurs along a surface as the surface changes velocities. It is known that, as a surface changes velocities in the supersonic and hypersonic range, pressure disturbance waves propagate from the surface to the shock wave, changing the strength of the shock wave. This results in an entropy interface. Subsequently, the pressure disturbance waves reflect between the shock wave, entropy interface, and surface until a new steady state is reached. There is a finite time lapse between the change in velocity and the arrival at a new steady state condition. The instability of some missiles during deceleration, a problem discussed by Force (1)*, has suggested that the pressure distribution may change with time and position along the missile to such an extent that the stability derivatives may be adversely affected.

Several studies have been made of this problem. Gardner, Ludloff and Reiche (2) used a perturbation potential theory on thin bodies and showed that the drag coefficient decreased as acceleration increased, the rate depending on Mach number and profile. The results were good only

---

*Numbers in parentheses following names refer to items in the Bibliography.

for small accelerations. Frankl (3) used retarded potential and small perturbation theory on elongated bodies of revolution and found that for velocities near the speed of sound, the added pressures arising from acceleration are negligibly small. Cole (4) used linearized theory of slender bodies and concentrated on the transonic range. It was shown that for sufficiently large accelerations, linearized theory is valid and there is little effect of acceleration on the pressure. Gardner and Ludloff (5) used a perturbation approach on slender two-dimensional airfoils, showing that the influence of acceleration in the supersonic range was very small but that in the transonic range, the pressure curve depended heavily on acceleration. Lighthill (6) used piston theory to determine the pressure distribution on an oscillating airfoil, but did not consider the reflections of the pressure disturbance waves from the shock wave. The theory developed by Lighthill could easily be extended to the case of accelerating or decelerating surfaces.

The purpose of this paper is to investigate the use of piston theory and the theory of characteristics, considering the effects of the entropy gradient across the attached shock, for the determination of the pressure distribution along an accelerating or decelerating flat plate at an angle of attack in the hypersonic and supersonic velocity regimes. A primary advantage of the piston theory method is the physical understanding it affords of the problem. In addition, only minor simplifying assumptions are necessary in the solution. For simplicity, the flat plate is used for the development herein. The principles could be extended, however, to surfaces with other shapes.

In Chapter II, the physical problem will be described and the general wave equations for the solution of the problem will be developed. In Chapter III, the hypersonic case will be considered and a numerical-graphical solution and an analytic solution will be presented. In Chapter IV, the supersonic case will be considered. For the most general case, or supersonic case, expressions will be developed for the matching of conditions which exist at a point on the shock wave where an incident and reflected wave and an entropy interface meet. A general discussion of the pressure disturbance wave pattern in the area between the flat plate and the shock wave will be presented.

Time would not permit a complete development of the theory of characteristics for the supersonic case. A discussion and some analysis for this case are included for record, however, in the belief that with additional effort, a practical solution can be developed.

Finally, as a result of the work on the hypersonic case, an extension of the work of Lighthill (6) will be presented in the appendix for the case of an oscillating flat plate.

CHAPTER II

THE PHYSICAL PROBLEM AND WAVE EQUATIONS

A physical appreciation of the general problem may be gained by picturing a flat plate, Figure 1(a), at an angle of attack, θ, traveling through a medium at some initial Mach number, M_1. Attached to the leading edge of the flat plate is a shock wave with a strength and angle to the horizontal, β, which is determined by the values of M_1 and θ.

The surface of the flat plate acts as a piston which moves in a direction perpendicular to the flat plate surface and induces a velocity of the medium in that direction. In addition, the fact that the shock wave is attached to the leading edge of the flat plate demands that there be a flow slippage, that is, a component of velocity tangent to the flat plate, in the area between the flat plate and the shock wave. The resultant flow velocity in this area is given by the equation

$$\frac{u_p}{a_1} = M_1 \frac{\text{Sin } \theta}{\text{Cos } \beta-\theta} \tag{1}$$

and acts in a direction perpendicular to the shock wave. The velocity of the plane shock wave is given by the expression

$$\frac{u_s}{a_1} = M_1 \text{ Sin } \beta \tag{2}$$

If the flat plate now undergoes either an impulsive acceleration or deceleration, it is necessary that the flow conditions between the flat plate and the shock wave undergo changes tending to adjust toward the new steady state conditions. As the acceleration or deceleration occurs, plane pressure disturbance waves parallel to the flat plate surface travel in a direction perpendicular to the flat plate surface out toward the shock wave. The disturbance wave will travel at a speed $u + a$ where u is the flow velocity in the direction of travel of the wave and a is the local speed of sound. This velocity is such that the disturbance wave will overtake and interact with the shock wave. The strength of the shock wave will be changed, an entropy interface will be created and a pressure disturbance wave will be reflected back toward the flat plate surface at some new angle.

As the pressure disturbance wave propagates, it causes a change in the component of flow velocity perpendicular to the wave. In the case of pressure disturbance waves, just as in the case of shock waves, the tangential component of velocity is not changed as it crosses the wave.

Subsequently, attenuated pressure disturbance waves will be reflected between the flat plate surface, the entropy interface and the shock wave until the new steady state condition corresponding to the new Mach number is reached. It is seen that there will be a finite time lapse between the time the flat plate reaches a new steady state velocity and the time the pressure reaches the new steady state pressure.

For the case of low supersonic velocities, the magnitude of the angle $(\beta - \theta)$ is appreciable and as illustrated in Figure 1 (a),

there is a considerable difference between the direction in which the original pressure disturbance wave propagates out to the shock wave and the direction in which the pressure disturbance wave is reflected. As the Mach number of the flat plate increases, however, the shock wave becomes more nearly parallel to the flat plate surface and the angle $(\beta - \theta)$ decreases. As hypersonic velocities are reached, the angle $(\beta - \theta)$ becomes small and the shock wave may be assumed parallel to the flat plate surface.

The significance of $(\beta - \theta)$ becoming small is that the component of flow velocity normal to the flat plate surface becomes essentially equal to the flow velocity since $\text{Cos}\ (\beta - \theta) \approx 1.0$. For instance, at $(\beta - \theta) = 10°$, only a 1.5 per cent error in the flow velocity results.

Also, as the Mach number increases, the angle between the propagating disturbance wave and the reflected disturbance wave becomes less, Figure 1 (b), until in the hypersonic case, Figure 1 (c), the propagated and reflected waves may be assumed to be parallel. The values of Mach number for which the hypersonic solution may be assumed will be more clearly defined in succeeding chapters.

From this physical description of the problem, it is seen that the acceleration or deceleration of a flat plate induces a network of plane wave motion in the area between the flat plate surface and the shock wave. In the remainder of this chapter, the general equations which describe such a plane wave motion are developed.

Following the development of Foa (7), use is made of the equations of continuity, motion and energy given below.

$$\frac{1}{\rho}\frac{\partial\rho}{\partial t} + \frac{u}{\rho}\frac{\partial\rho}{\partial x} + \frac{\partial u}{\partial x} = 0 \tag{3}$$

$$\frac{\partial u}{\partial t} + u\frac{\partial u}{\partial x} = -\frac{a^2}{\gamma p}\frac{\partial p}{\partial x} \tag{4}$$

$$d \ln \rho = \frac{2}{\gamma-1}\frac{da}{a} - \frac{ds}{R} \tag{5a}$$

$$d \ln p = \frac{2\gamma}{\gamma-1}\frac{da}{a} - \frac{ds}{R} \tag{5b}$$

where the energy equation, given by the first law of thermodynamics, is expressed in the two forms given by equations (5a) and (5b). Eliminating ρ between equations (3) and (5a), and eliminating p between equations (4) and (5b), and adding and subtracting the results gives

$$\frac{\partial}{\partial t}\left(\frac{2}{\gamma-1}a \pm u\right) + (u \pm a)\frac{\partial}{\partial x}\left(\frac{2}{\gamma-1}a \pm u\right) = \frac{a}{R}\left(\frac{Ds}{Dt} \pm \frac{a}{\gamma}\frac{\partial s}{\partial x}\right) \tag{6}$$

where viscosity has been neglected, area has been assumed constant and $\frac{D}{Dt}$ denotes the substantial derivative.

Equations (6) are nonlinear partial differential equations with their left hand sides being the total time derivatives of the functions $\left(\frac{2}{\gamma-1}a \pm u\right)$ in the directions $\frac{dx}{dt} = u \pm a$.

The equations may then be numerically integrated along lines of this slope in the x-t plane and these lines and the particle path lines $dx/dt = u$, which are also the entropy path lines, are called characteristics of equations (6). The speeds $dx/dt = u \pm a$ are recognized as the speeds of propagation of small disturbances. Characteristics of slope $dx/dt = u \pm a$ are paths of propagation of the disturbances in the x-t plane.

It will be convenient to non-dimensionalize equations (6) by making the following substitutions where the subscript 1 denotes conditions in front of the shock wave and D_{s_o} represents the initial distance from the piston to the shock at any arbitrary point along the flat plate.

$$A = a/a_1 \qquad \epsilon = x/D_{s_o}$$

$$U = u/a_1 \qquad \tau = a_1 t/D_{s_o}$$

$$S = s/\gamma R \qquad P = \frac{2}{\gamma-1} A + U$$

$$Q = \frac{2}{\gamma-1} A - U$$

If $\frac{\delta\pm}{\delta t}$ denotes differentiation with respect to time along the characteristics, that is, the operation $\frac{\partial}{\partial t} + (u \pm a) \frac{\partial}{\partial x}$, and if it is noted that $\frac{\delta\pm}{\delta t} = \frac{D}{Dt} \pm a \frac{\partial}{\partial x}$, equations (6) may be written in the form

$$\frac{\delta + P}{\delta \tau} = A \frac{\delta + S}{\delta \tau} + (\gamma-1) A \frac{DS}{D\tau} \tag{7}$$

$$\frac{\delta - Q}{\delta \tau} = A \frac{\delta - S}{\delta \tau} + (\gamma-1) A \frac{DS}{D\tau} \tag{8}$$

Equation (7) gives the rate of change of the variable P along the P characteristic $\frac{d\epsilon}{d\tau} = U + A$ and equation (8) establishes the rate of change of the variable Q along the Q characteristic $\frac{d\epsilon}{d\tau} = U - A$. It is well to point out here, that if P and Q are known at any point, the values of A and U are also known at that point and thus, the slope of the P and Q characteristics are established.

Equations (7) and (8) are general equations which describe unsteady plane wave motion such as exists as a result of the deceleration or acceleration of the flat plate and the corresponding deceleration or acceleration of the simulated piston. While these equations could be numerically integrated to solve for the flow field and pressure distribution for the flat plate for either the supersonic or hypersonic case, their use in the supersonic case is extremely complicated because of the complex wave network involved. Their use in the hypersonic case is simplified, however, and will be demonstrated in the next chapter.

CHAPTER III

HYPERSONIC CASE

In the preceeding chapter, equations were developed which described the plane wave motion such as would exist as a result of an acceleration or deceleration of a piston face. In this chapter, the use of these equations will be demonstrated for the determination of the pressure distribution along a decelerating flat plate traveling at hypersonic velocities. The angle, $(\beta - \theta)$, will be assumed to be nearly zero so that the shock wave is essentially parallel to the wedge surface and the propagated and reflected pressure disturbance waves are essentially parallel, Figure 1 (c).

As will be illustrated, the use of equations (7) and (8) requires time-consuming calculations carrying a large number of significant figures. Therefore, in the second part of this chapter, an analytic expression will be developed for the pressure distribution along the accelerating or decelerating flat plate after any number of disturbance wave reflections.

Finally, an equation representing the time necessary for the pressure disturbance wave to propagate from the piston surface to the shock wave and back to the piston surface will be presented. The range of hypersonic velocities for which either of these two solutions may be used will be determined.

A. Numerical-Graphical Solution.--To illustrate the determination of the pressure distribution along a decelerating flat plate at an angle

of attack by means of the numerical integration of equations (7) and (8), the instantaneous deceleration of the flat plate from some initial Mach number, M_1, to some final Mach number, M_2, and the corresponding deceleration of the simulated piston surface is considered. The time-distance plot for this situation is illustrated in Figure 2. The path of the piston is portrayed by the solid line starting from the origin and the instantaneous deceleration takes place at point A. Since x/D_{s_o} is plotted versus $a_1 t/D_{s_o}$, the shock wave will be at $x/D_{s_o} = 1.0$ and the piston surface at $x/D_{s_o} = 0$ at time $t = 0$. The convenience of the non-dimensionalizing parameters defined in Chapter II is now apparent. The solution obtained can be made to apply to any point along the surface by choosing the appropriate value for D_{s_o}. The solution will also apply for any value of a_1.

Until the deceleration takes place at point A, the conditions are steady. Knowing the piston velocity from equation (1), where Cos $(\beta - \theta) \approx 1.0$, and knowing from shock tables the speed of sound ratio corresponding to the shock Mach number obtained from equation (2), the values of P and Q and the slopes of the P and Q characteristics may be obtained in this steady state area. Since, in this area, the flow is isentropic, and U and A are constant, P and Q are constant along P and Q characteristics of slope $\frac{d\epsilon}{d\tau} = U \pm A$ respectively. Equations (7) and (8) show that in any area where conditions are isentropic, P and Q are constant along characteristic lines of slope $\frac{d\epsilon}{d\tau} = U \pm A$. Area 2, Figure 2, includes the entire area between the piston curve and the entropy interface and represents an area of constant entropy. Therefore, P and Q are constant along the P and Q characteristics in this

area. Likewise, area 3 represents an area of constant entropy between the entropy interface and the shock wave and P and Q are also constant along P and Q characteristics in this area.

At point A, where the piston velocity changes, there is also a change in the variable P. At Point A, Q is a constant. Therefore,

$$dQ = 0 = \frac{2}{\gamma-1} dA - dU \tag{9}$$

and

$$dP = \frac{2}{\gamma-1} dA + dU = 2dU \tag{10}$$

which for a deceleration would make dP negative. Knowing the new value of P at point A and the value of Q which still has its steady state value, the new value of the variable A existing immediately after the deceleration may be obtained along with the slope of the new P characteristic emanating from this point.

It is emphasized that there is actually a fan of P characteristics emanating from point A, each with its corresponding value of the variable P. The pressure solution is not affected by considering a finite step. However, a need for greater accuracy in the time solution would dictate that this fan be broken up into intervals and further calculations continued on this basis. Working with the total increment, though, makes the calculations far simpler and is felt to yield sufficient accuracy, particularly if small enough steps are taken in the deceleration.

As a result of the deceleration, pressure expansion disturbance waves travel along the P characteristic in the ϵ- τ plane and overtake the shock wave, shown by the dot-dash line in Figure 2, causing a change in strength of the shock wave. Since the flow properties and conditions

after the disturbance waves are not compatible with a shock solution, a wave is reflected at the shock as a Q wave traveling along Q characteristics. Furthermore, an entropy interface is created as the shock strength changes. Although there is a gradual change in shock strength between the points where the initial and final P disturbances emanating from point A strike the shock, the change in shock strength is assumed to occur at a point midway between the two points and the entropy interface is assumed to emanate from that point.

The numerical value of the Q wave emanating from point B is still the same as the steady state value, that is, the entropy has remained constant. Knowing this value and the value of P at point B, the slope of this Q characteristic may be computed at the shock and its point of intersection with the P characteristic. Its intersection with the piston face at point C may then be determined.

As P changes between points B and D, Q also changes. As illustrated in Figure 2, the P_{b2} wave passes through an entropy interface and strikes the shock wave. In order to make conditions compatible at this point, a Q wave originates which passes back through the entropy interface and travels on to the piston face. The only condition known near point D is the value of the P_{b2} wave before it strikes the entropy interface at D'. It is, therefore, necessary to iterate at this point in order to find the value of the Q_{b2} wave which is also assumed to meet the entropy interface at point D'.

This iteration is performed by assuming initially, a value of M_s, the new Mach number at which the shock wave is propagating. Knowing M_s, the value of M_3 and a_3/a_1 can be obtained from shock tables, and, from these two quantities, the value of u_3/a_1 is determined. The subscript 3, in this case, refers to the area between the entropy interface

and the shock wave at point D. The value of u_p/a_1 in area 3 at point D is obtained by subtracting u_3/a_1 from the assumed u_s/a_1.

It is known that the entropy interface travels at the same speed as the local flow velocity and that the pressures on the two sides of the entropy interface must be equal. The value of U, then, must be the same in area 2 at D' as it is in area 3 at D'. It remains to solve for the value of A in area 2 knowing the value of A in area 3.

The entropy in areas 2 and 3 may be related to the entropy in area 1 by the following equations.

$$\frac{s_3 - s_1}{c_p(\gamma-1)} = \frac{2}{\gamma-1} \ln A_3 - \frac{1}{\gamma} \ln \frac{p_3}{p_1} \tag{11}$$

$$\frac{s_2 - s_1}{c_p(\gamma-1)} = \frac{2}{\gamma-1} \ln A_2 - \frac{1}{\gamma} \ln \frac{p_2}{p_1} \tag{12}$$

Since $p_2 = p_3$ across the entropy interface. equation (12) can be subtracted from equation (11) and the result solved for A_3/A_2 obtaining

$$\frac{A_3}{A_2} = \exp\left[\frac{s_3 - s_2}{2c_p}\right] \tag{13}$$

The values of A and U in area 2 at D' are now known and a value for P_{b2} can be computed. If the calculated value equals the existing value of P_{b2}, conditions have been successfully matched at point D'. If not, a new value of M_s is assumed and the iteration is continued until conditions are matched. Once the correct values of A and U are known in area 2 at D', the value of Q and the slope of the Q characteristic can be computed and the intersection of the Q characteristic with the piston

face at point E determined. At the same time, the value of Q in area 3 at D' is determined from the above iteration.

At points C and E the values of the variable Q and the piston velocity U are known. The values of the P wave reflected at these points may be calculated, together with the values of the slopes of the P characteristics. The P waves reflected at points C and E travel out and strike the entropy interface, where they are partially passed through and partially reflected back toward the piston face as Q waves. At the same time, Q waves in area 3, known from the iteration outlined above, travel from the shock to the entropy discontinuity and are partially passed through and partially reflected as P waves back toward the shock. Again, at the entropy interface, points F and G, conditions must be matched. This time, however, the matching may be accomplished in closed form.

For example, at point G, the values of Q_{d_3} and P_{d_2} are known and the values of U and p on either side of the entropy interface are again equal. Then

$$P_{d2} = \frac{2}{\gamma-1} A_2 + U_2 \tag{14}$$

$$Q_{d3} = \frac{2}{\gamma-1} A_3 - U_3 \tag{15}$$

Adding equations (14) and (15),

$$P_{d2} + Q_{d3} = \frac{2}{\gamma-1} (A_2 + A_3) \tag{16}$$

Using this equation together with equation (13), A_2 and A_3 at G are

found, U_2 and U_3 are solved for and Q_{d2} and P_{d3} together with the slopes of the characteristics at point G are determined.

To complete the solution of the problem, new reflections of the disturbance waves are considered until there is no significant change in the value of the P or Q variables and a new steady state is reached.

At each point along the piston face where a P and Q wave intersect, the value of $A = a/a_1$ is known. Since the entropy is constant in the region of the piston face, the pressure ratio at each of these points may be obtained from the isentropic expression

$$\frac{p}{p_1} = \left(\frac{p_2}{p_1}\right)_o \left[\frac{a/a_1}{(a_2/a_1)_o}\right]^{\frac{2\gamma}{\gamma-1}} \tag{17}$$

where the initial values of p_2/p_1 and a_2/a_1 are obtained from the shock tables.

The motion of the effective piston face and the variation of pressure with the ordinate a_1t/D_{s_o} are now known. It must be recognized here that as the flat plate moves through the air, a section of the flat plate surface, considered as a piston face, moves aft along the flat plate surface and translates in the x direction as illustrated in Figure 3 (a). The relation between these two motions is obtained in terms of the initial distance from the flat plate to the shock wave, D_{s_o}, and the angles β and θ by considering Figure 3.

From Figure 3 (a), it is seem that

$$y_o = y - \frac{x}{\tan \theta} \tag{18}$$

From Figure 3 (b), it is found that

$$y_o = \frac{D_{s_o}}{\tan(\beta - \theta)} \tag{19}$$

Equating these two expressions for y_o gives

$$\frac{D_{s_o}}{y} = \left[1 - \frac{x}{y} \frac{1}{\tan \theta}\right] \tan(\beta - \theta) \tag{20}$$

The relationship of the flat plate surface to a simulated piston moving through space has now been developed. In addition, the method for determining the pressure distribution on the simulated piston face has been presented. It remains to combine the results so that the pressure distribution along the flat plate may be obtained.

Two plots of the pressure distribution along the flat plate would be of interest. One plot would show pressure as a function of time at any position y along the flat plate. The second plot of interest would show pressure versus distance y along the flat plate at any time t. The two plots may be combined by plotting pressure distribution versus the dimensionless parameter $a_1 t/y$. This is done as follows.

The angles θ and β are known for any case under consideration. If various values for x/y are assumed, values for D_{s_o}/y are obtained from equation (20). From these two values, a value of x/D_{s_o}, is computed. Knowing the motion of the piston, x/D_{s_o}, as a function of the parameter τ, a value of τ corresponding to the computed value of x/D_{s_o} may be determined. Also, at this same value of τ, the value of the pressure ratio may be found from a plot of the pressure ratio versus τ.

Finally, knowing ta_1/D_{s_o}, x/y, and D_{s_o}/x, the parameter ta_1/y may be determined and a plot of pressure ratio versus a_1t/y may be made.

To illustrate the above procedures, a sample problem was computed using a flat plate at an angle of attack $\theta = 10°$, decelerating from $M_1 = 6.0$ to $M_2 = 5.0$. In the sample problem, the effective piston velocity was determined from equation (1), where Cos $(\beta - \theta)$ was not taken equal to 1.0. Other values in the solution, however, were determined as outlined above. Plots of the ϵ-τ plane, pressure ratio versus τ, and pressure ratio versus a_1t/y are shown in Figures 4, 5, and 6. The pressure coefficient used is given by

$$C_p = \frac{p_{M=6} - p}{p_{M=6} - p_{M=5}}$$

where $p_{M=6}$ is the steady state pressure at $M = 6.0$ and $p_{M=5}$ is the steady state pressure at $M = 5.0$.

It is seen from Figure 6, that the pressure on the flat plate immediately after the deceleration is considerably less than the steady state pressure at $M_2 = 5.0$. However, the first reflection of the disturbance waves from the shock wave to the flat plate surface is seen to account for the major correction of the pressure back toward the steady state value. It is also noted that there is one reflection of the pressure disturbance wave from the entropy interface before the second reflection from the shock wave takes place. This reflection has little effect, however, on the pressure solution. Finally, it is pointed out that this single plot illustrates the variation in pressure with time for a fixed position if y is held constant and the variation of pressure with position if t is held constant. With practical values of y, the time

to establish the new steady state pressure is measured in milliseconds. For example, if $y = 10$ feet and $a_1 = 1000$ feet per second, steady state is essentially reached in 1.9 milliseconds.

The method outlined above can be readily extended to a flat plate undergoing linear or non-linear accelerations or decelerations. For example, results for a particular continuous deceleration can be readily obtained from the preceeding results by a simple geometric adjustment of the network of Figure 4. Imagine that a streamline between points A and B is replaced by the surface. The surface deceleration then occurs over a finite time interval and the scale adjustment is made by simply translating the subsequent P and Q characteristics such that points C, E, H, I, L and M intersect the new surface.

In addition, the method can be extended to cover shapes other than the flat plate. However, it will be noted by the reader that to perform the calculations by hand requires many computations. Furthermore, the single case considered illustrates that several significant figures must be carried in order to assure reasonable accuracy. In fact, available shock tables have an insufficient number of significant figures. Although it is possible to machine program the method, considerable effort would be required and it is felt to be beyond the scope of this paper.

Attention is now turned to the development of an analytic expression for the pressure distribution along the flat plate and to the development of an equation for the time lag which exists between the time the deceleration or acceleration takes place and the time the reflected disturbance wave strikes the piston face.

B. Analytic Solution.--As the deceleration or acceleration takes place an expansion or compression pressure disturbance wave immediately propagates from the flat plate surface out toward the shock wave. There is a resulting immediate change in the pressure along the surface which can be expressed analytically.

Starting with the condition that initially the variable Q remains constant as the surface velocity changes, equation (9) gives

$$dA = d\,\frac{a}{a_1} = \frac{\gamma-1}{2}\,dU \tag{21}$$

From equation (1), where Cos $(\beta - \theta) \approx 1.0$ for the hypersonic case,

$$d\,\frac{u}{a_1} = dU = \sin\theta\,dM_1 \tag{22}$$

Combining equations (21) and (22),

$$dA = \frac{\gamma-1}{2}\,\mathrm{Sin}\,\theta\,dM_1 \tag{23}$$

For isentropic conditions which exist along the flat plate surface,

$$\frac{a}{a_1} = \left(\frac{p}{p_1}\right)^{\frac{\gamma-1}{2\gamma}} \tag{24}$$

or

$$\frac{d\,\frac{a}{a_1}}{a/a_1} = \frac{\gamma-1}{2\gamma}\,\frac{d\,p/p_1}{p/p_1} \tag{25}$$

Substituting equation (25) into equation (23),

$$d\,\frac{p}{p_1} = \frac{\gamma\ p/p_1}{a/a_1}\ \sin\theta\ dM_1 \tag{26}$$

Changing dM_1 to $dM_1^{\,2}/2M_1$ for later convenience and noting that p/p_1 and a/a_1 are the initial steady state values, the following expression for the change in pressure ratio with respect to $M_1^{\,2}$ resulting immediately after an acceleration or deceleration is obtained.

$$\frac{d\,\frac{p}{p_1}}{dM_1^{\,2}} = \frac{\gamma(p_2/p_1)_o\ \mathrm{Sin}\ \theta}{2\ M_1(a_2/a_1)_o} \tag{27}$$

The initial surface velocity change generates a P wave propagating from the flat plate surface to the shock. Corresponding to this P wave intersecting the shock wave, there is a Q wave reflecting from the shock wave. This reflected Q wave strikes the flat plate surface, changing the surface pressure and reflecting as a P wave. It remains to express this reflected Q wave as a function of the P wave and then to arrive at an expression for a corresponding change in pressure.

First, considering changes across the shock wave, Figure 7, the following relations from Liepmann and Roshko (8) apply.

$$\frac{u_p}{a_1} = \frac{1}{\gamma}\left(\frac{p_2}{p_1} - 1\right)\frac{\frac{2\gamma}{\gamma-1}}{\left(\frac{p_2}{p_1} + \frac{\gamma-1}{\gamma+1}\right)^{1/2}} \tag{28}$$

and

$$\frac{a_2}{a_1} = \left(\frac{p_2}{p_1}\right)^{1/2} \frac{\left(\frac{\gamma+1}{\gamma-1} + \frac{p_2}{p_1}\right)^{1/2}}{\left(1 + \frac{\gamma+1}{\gamma-1}\frac{p_2}{p_1}\right)^{1/2}} \tag{29}$$

Now let subscript 3, $(\ )_3$, represent conditions immediately downstream of the shock wave.

From equation (28)

$$d\,\frac{u_{p_3}}{a_1} = f_1\left[\left(\frac{p_2}{p_1}\right)_o\right] d\,\frac{p_3}{p_1} \tag{30}$$

where

$$f_1 = f_1\left[\left(\frac{p_2}{p_1}\right)_o\right] = \frac{\left(\frac{2\gamma}{\gamma+1}\right)^{1/2}\left[\left(\frac{p_2}{p_1}\right)_o + \frac{3\gamma-1}{\gamma+1}\right]}{2\gamma\left[\left(\frac{p_2}{p_1}\right)_o + \frac{\gamma-1}{\gamma+1}\right]^{3/2}} \tag{31}$$

From equation (29)

$$d\,\frac{a_3}{a_1} = f_2\left[\left(\frac{p_2}{p_1}\right)_o\right] d\,\frac{p_3}{p_1} \tag{32}$$

where

$$f_2 = f_2\left[\left(\frac{p_2}{p_1}\right)_o\right] = \frac{1}{2}\left(\frac{a_2}{a_1}\right)_o \left[\frac{1}{\left(\frac{p_2}{p_1}\right)_o} + \frac{1}{\frac{\gamma+1}{\gamma-1} + \left(\frac{p_2}{p_1}\right)_o} - \frac{\frac{\gamma+1}{\gamma-1}}{1 + \frac{\gamma+1}{\gamma-1}\left(\frac{p_2}{p_1}\right)_o}\right] \tag{33}$$

In equations (31) and (33), the functions f_1 and f_2 are expressed in terms of $(p_2/p_1)_o$ and $(a_2/a_1)_o$ since for an infinitesimal disturbance, $(p_2/p_1)_o$ and $(a_2/a_1)_o$ becomes exactly equal to p_3/p_1 and a_3/a_1. From equations (30) and (32), it is seen that

$$d\ \frac{a_3}{a_1} = \frac{f_2}{f_1}\ d\ \frac{u_{p_3}}{a_1} \tag{34}$$

Also in area 3, the entropy is known from the following expression

$$S_3 - S_1 = \frac{2}{\gamma-1} \ln \frac{a_3}{a_1} - \frac{1}{\gamma} \ln \frac{p_3}{p_1} \tag{35}$$

where S_1 is a constant.

From equation (35), making use of the functions f_1 and f_2,

$$dS_3 = \left[\frac{2}{\gamma-1}\ \frac{f_2}{f_1}\ \frac{1}{\left(\frac{a_2}{a_1}\right)_o} - \frac{1}{\gamma\ f_1\left(\frac{p_2}{p_1}\right)_o} \right] d\ \frac{u_{p_3}}{a_1} \tag{36}$$

Now, if region 2 is considered, it is known from equation (10) that

$$P_{b2} - P_{a2} = \Delta P = 2\Delta\ \frac{u_{p_A}}{a_1} \tag{37}$$

Also, from definition, it is known that

$$P_{b2} - P_{a2} = \left(\frac{2}{\gamma-1}\ \frac{a_{b2}}{a_1} + \frac{u_{b2}}{a_1}\right) - \left(\frac{2}{\gamma-1}\ \frac{a_{a2}}{a_1} + \frac{u_{a2}}{a_1}\right) \tag{38}$$

$$Q_{b2} - Q_{a2} = \left(\frac{2}{\gamma-1}\ \frac{a_{b2}}{a_1} - \frac{u_{b2}}{a_1}\right) - \left(\frac{2}{\gamma-1}\ \frac{a_{a2}}{a_1} - \frac{u_{a2}}{a_1}\right) \tag{39}$$

Since the piston velocity on either side of the entropy discontinuity is the same, $u_{a2} = u_{a3}$, and $u_{b2} = u_{b3}$. Subtracting one from the other and dividing by a_1,

$$\frac{u_{b2}}{a_1} - \frac{u_{a2}}{a_1} = \frac{u_{b3}}{a_1} - \frac{u_{a3}}{a_1} = \Delta\left(\frac{u_{p3}}{a_1}\right) \tag{40}$$

and equations (38) and (39) become

$$P_{b2} - P_{a2} = \frac{2}{\gamma-1}\left(\frac{a_{b2} - a_{a2}}{a_1}\right) + \Delta\,\frac{u_{p3}}{a_1} \tag{41}$$

$$Q_{b2} - Q_{a2} = \frac{2}{\gamma-1}\left(\frac{a_{b2} - a_{a2}}{a_1}\right) - \Delta\,\frac{u_{p3}}{a_1} \tag{42}$$

Subtracting and rearranging equations (41) and (42),

$$Q_{b2} - Q_{a2} = (P_{b2} - P_{a2}) - 2\Delta\left(\frac{u_{p3}}{a_1}\right) \tag{43}$$

Across the entropy interface where the pressures on either side are equal, equation (35) may be differentiated and expressed as a finite difference equation to yield,

$$\Delta S_3 = \frac{2}{\gamma-1}\ \frac{\Delta a/a_1}{(a_2/a_1)_o} = \frac{2}{\gamma-1}\ \frac{\left(\dfrac{a_{b3} - a_{b2}}{a_1}\right)}{(a_2/a_1)_o} \tag{44}$$

Recognizing that $a_{a2} = a_{a3}$, $\dfrac{(a_{b2} - a_{a2})}{a_1}$ from equations (41) and (42)

may be expressed as

$$\frac{a_{b2} - a_{a2}}{a_1} = \frac{a_{b2} - a_{b3} + a_{b3} - a_{a2}}{a_1} = - \frac{a_{b3} - a_{b2}}{a_1} + \frac{a_{b3} - a_{a3}}{a_1} \tag{45}$$

Making equations (34) and (36) finite difference equations and substituting these along with equation (44) into equation (45), the following expression is obtained.

$$\frac{a_{b2} - a_{a2}}{a_1} = - \frac{\gamma-1}{2}\left(\frac{a_2}{a_1}\right)_o \left[\frac{2}{\gamma-1} \frac{f_2}{f_1} \frac{1}{\left(\frac{a_2}{a_1}\right)_o} - \frac{1}{\gamma f_1\left(\frac{p_2}{p_1}\right)_o} - \frac{f_2}{f_1}\right] \Delta \frac{u_{p3}}{a_1} \tag{46}$$

Substituting equation (46) into equation (41), solving for $\Delta \frac{u_{p3}}{a_1}$ and substituting this expression into equation (43), an expression is finally obtained for the Q wave as a function of the P wave. Taking the limiting case and converting to differentials, the expression becomes

$$(dQ)_1 = dP\left(F \right) \tag{47}$$

where

$$\left(F \right) = 1 - \frac{2}{\frac{(a_2/a_1)_o}{\gamma f_1 (p_2/p_1)_o} + 1} \tag{48}$$

The subscript 1 refers to the first reflection from the shock.

This Q wave strikes the flat plate surface, causing a resultant

change in pressure. The effect of this Q wave on the surface pressure is now obtained by holding the piston velocity constant during the surface-wave interaction. Therefore

$$dQ = \frac{2}{\gamma-1} dA = \frac{2}{\gamma-1} d \frac{a}{a_1} \tag{49}$$

Substituting equations (49), (10), (22), and (25) into equation (47), the pressure ratio change with respect to M_1^2 for the first reflection becomes

$$\left(\frac{d \frac{p}{p_1}}{dM_1^2}\right)_1 = \frac{\gamma(p_2/p_1)_o \sin \theta}{(a_2/a_1)_o M_1} \left(F \right) \tag{50}$$

It is recognized that the dQ which results from the first reflection at the shock is reflected from the flat plate surface as a P wave, where the reflected dP equals the incident dQ. Thus, again employing the above results, the dQ for the second reflection is given by

$$(dQ)_2 = dP \left(F \right)^2 \tag{51}$$

and this same reasoning may be carried on to succeeding reflections. Thus, the total change in pressure with respect to M_1^2 may be obtained by adding the original pressure change, equation (27), to the pressure change resulting from the reflections and the final expression becomes

$$\left(\frac{d \frac{p}{p_1}}{dM_1^2}\right)_n = \frac{\gamma(p_2/p_1)_o \operatorname{Sin} \theta}{(a_2/a_1)_o M_1} \left[\frac{1}{2} + F + F^2 + \ldots + F^n \right] \tag{52}$$

where n is the number of reflections considered.

Equation (52) expresses the surface pressure change for n reflections following an infinitesimal velocity change. However, assuming that linearized theory holds within the region between the shock and surface, the differentials can be replaced by finite differences, that is, it can be assumed that $\frac{\gamma(p_2/p_1)_o}{(a_2/a_1)_o M_1}$ and F are approximately constant during the time required for the significant reflections to occur. As will be shown subsequently, changes occurring during decelerations or accelerations which occur at reasonable rates are sufficiently small so that the linearized theory is justified in most cases.

As a basis for evaluating the above equation, and illustrating the effects of reflected waves, a direct comparison to steady state shock solutions can be made. The pressure change across an oblique shock is given by

$$\frac{p_2 - p_1}{p_1} = \frac{2\gamma}{\gamma+1} \left(M_1^2 \operatorname{Sin}^2 \beta - 1\right) \tag{53}$$

In addition, the equation giving the relation between θ, M_1, and β is

$$\tan \theta = 2 \operatorname{Cot} \beta \; \frac{M_1^2 \operatorname{Sin}^2 \beta - 1}{M_1^2(\gamma + \operatorname{Cos} 2\beta) + 2} \tag{54}$$

Letting $M_1^2 \operatorname{Sin}^2 \beta = Z$, the derivative of both sides of equation (53) is taken with respect to M_1^2, obtaining

$$\frac{d \frac{p_2}{p_1}}{dM_1^2} = \frac{2\gamma}{\gamma+1} \frac{dZ}{dM_1^2} \tag{55}$$

Then, with θ constant, the derivative of both sides of equation (54) is taken with respect to M_1^2 and the resulting expression solved for dZ/dM_1^2. Substituting this expression for dZ/dM_1^2 into equation (55), letting $\gamma = 1.4$ and simplifying, the following expression is obtained

$$\frac{d\,\frac{p_2}{p_1}}{dM_1^2} = \frac{2.8}{2.4}\left\{\frac{\left[(-.7Z^2 + .2Z + .5) + .6M_1^2(Z-1)\right]Z}{M_1^2(-.7Z^2 - 1.0Z + .5) + .6M_1^4(Z+1) - .5(Z-1)}\right\} \qquad (56)$$

This expression gives the exact change in steady state pressure ratio across an oblique shock for a change in M_1^2.

Figures 8, 9, and 10 show a plot of $\frac{d\,p_2/p_1}{dM_1^2}$ obtained from the theory, equation (52), divided by the value of $\frac{d\,p_2/p_1}{dM_1^2}$ from equation (56) versus Mach number and the angle $(\beta - \theta)$. These results illustrate the effect of differential or linearized step changes in Mach number on the surface pressure lag, that is, the effect of wave reflections on the corresponding surface pressure lag. Furthermore, they directly demonstrate the accuracy of the unsteady flow, hypersonic theory since the ordinate should approach 1.0 when the number of reflections becomes large.

In Figures 8 (a), 9 (a), and 10 (a), the abscissa is the angle between the flat plate and the shock wave, $(\beta - \theta)$. This choice is dictated by the fact that the accuracy of the hypersonic piston theory is dependent upon the approximation that $\cos(\beta - \theta) \approx 1.0$, as previously discussed. Thus, it is expected that this plot should correlate results reasonably well regardless of M_1 or the angle θ. It can also be shown

that the angle $(\beta - \theta)$ is essentially dependent only upon M_1 for ranges of M_1 and θ of most interest. Since M_1 is a more convenient and descriptive parameter, the results plotted in Figures 8 (b), 9 (b), and 10 (b) employ M_1 as the abscissa.

The plot of the pressure ratio versus $(\beta - \theta)$ and M_1 for no wave reflections, that is, the pressure ratio existing immediately after a change in velocities, is presented in Figure 8. This corresponds to the so-called shock expansion theory and it can be seen that there is considerable error, particularly at the higher Mach numbers.

Shown in Figures 9 and 10 are the pressure ratio curves for one and two reflections of the pressure disturbance waves. It is seen that the first reflection again accounts for the major correction of the pressure back toward steady state values. The first reflection results in a pressure ratio within one per cent of steady state value for M_1 greater than 5.60. The second reflection makes a further non-negligible correction to the pressure ratio, but, succeeding reflections have little effect.

The solid lines of Figures 8, 9, and 10 were computed for $\theta = 10°$. In order to illustrate the effect of θ, however, one calculation was made with $\theta = 15°$ and two calculations were made with $\theta = 20°$ for values of $(\beta - \theta)$ and M_1 near the limits of good accuracy. These points are plotted on Figures 9 and 10, illustrating that good correlation is obtained with the solid curves for the cases of one and two reflections.

Figure 9 shows that if one reflection is considered, this hypersonic theory will result in accuracy within one per cent for values of M between 5.6 and 11.7. If two reflections are considered, the theory gives

an accuracy within one per cent for values of M greater than 5.8 with no apparent upper limit on M. It is interesting to note that the theory apparently results in about the same degree of accuracy for values of θ up to at least 20°.

It was pointed out earlier that in the steady state case, the flow velocity between the flat plate and shock wave was in a direction perpendicular to the shock wave. When a change in velocity of the flat plate occurs, there is a resultant change in piston velocity perpendicular to the flat plate which has a component perpendicular to the shock of

$$\frac{du_p}{a_1} = \sin\theta \cos(\beta - \theta)\, dM_1 \tag{57}$$

It is this component of the change in flow velocity which one might expect to be of significance in establishing the pressure change.

If the rotation of the shock, that is, the change in $(\beta - \theta)$, is negligible, a modified piston theory is obtained by multiplying equation (52) by the factor $\cos(\beta - \theta)$. The plot of the pressure ratio versus M_1 and $(\beta - \theta)$ for two reflections using this modified theory is presented in Figure 11. This Figure shows that the modification extends the theory so that good accuracy is obtained for considerably lower values of M. Correlation is still shown to be good for values of θ of 15° and 20°. It is important to point out, however, that this approach neglects the effect of the component of initial velocity perturbation tangential to the shock wave. That is, if the theory accurately predicts the steady state surface pressure after several reflections, this

tangential component must necessarily be attenuated. Since this component is initially neglected, the time-pressure variations associated with this attenuation process are neglected.

The preceding comparisons illustrate the limits of applicability of the small perturbation or linearized theory which has been developed. It remains, however, to establish the corresponding time-pressure relationship for acceleration or deceleration and to investigate the extent to which the small perturbation or linearized theory may be applied.

To determine the time involved for the pressure disturbance wave to travel from the flat plate to the shock wave and back to the flat plate after a change in flat plate velocities, consider Figure 12. If Δt_1 is the time it takes for the disturbance wave to travel from the piston to the shock wave, then during this time the shock wave moves

$$D_1 = u_s \Delta t_1 \tag{58}$$

and the pressure disturbance wave moves

$$D_1 + D_{s_o} = (u + a) \Delta t_1 \tag{59}$$

During the time Δt_1 described above and the time Δt_2 which it takes the disturbance wave to travel from the shock wave to the flat plate, the piston travels a distance

$$D_2 = u_p (\Delta t_1 + \Delta t_2) \tag{60}$$

Also, during time Δt_2, the disturbance wave travels a distance

$$D_1 + D_s - D_2 = (u_p - a) \Delta t_2 \tag{61}$$

Equations (58), (59), (60), and (61) may be solved for the time $\eta = \Delta t_1 + \Delta t_2$ in terms of u_p, u_s, a, a_1 and D_{s_o} giving

$$\frac{a_1\eta}{D_{s_o}} = \frac{2\,\frac{u_p}{a_1}}{\left(2\,\frac{u_p}{a_1} - \frac{a}{a_1}\right)\left(\frac{u_p}{a_1} + \frac{a}{a_1} - \frac{u_s}{a_1}\right)} \tag{62}$$

The expression has been made non-dimensional so that the parameter $\frac{a_1\eta}{D_{s_o}}$ is independent of position along the plate. This equation represents the time lapse from the initial change in velocity and surface pressure until the first reflection strikes the flat plate resulting in the second pressure change along the flat plate surface. Equation (62) would also be applicable for the second, third and subsequent reflections. In fact, it can readily be converted to a single equation for the general case of n reflections.

A plot of $\frac{a_1\eta}{D_{s_o}}$ versus M_1 is included as Figure 13 for the same values of M_1 for which equation (52) is assumed accurate. It is noted again, assuming realistic values for a_1 and D_{s_o}, that this time lapse is measured in milliseconds.

Equation 62 can now be utilized to illustrate the rate at which disturbances are reflected for reasonable values of the parameters and, thus, to justify the utilization of small perturbation or linearized theory. The criterion is that the relative change in flow velocity ahead of the flat plate over the interval of time required for the effects of the change to be attenuated must be small. This can be stated by

$$\frac{du_p}{dt}\ \frac{\eta}{u_p} = \frac{du}{dt}\ \frac{\eta}{u} = \delta << 1.0 \tag{63}$$

This can be written as

$$\frac{du}{dt}\ \frac{\eta}{u} = \frac{\frac{du}{dt}\ D_{s_o}}{M_1\ a_1^2}\left[\frac{a_1\eta}{D_{s_o}}\right] = \delta \tag{64}$$

or

$$\frac{y}{(a_1/1000)^2}\ \frac{\frac{du}{dt}}{g_o} = \frac{\delta M}{g_o\ \frac{a_1\eta}{D_{s_o}}}\ \frac{y}{D_{s_o}} = \frac{\delta M\ \mathrm{Cot}\ (\beta - \theta)}{g_o\ \frac{a_1\eta}{D_{s_o}}} \tag{65}$$

where the acceleration du/dt is normalized by the standard acceleration due to gravity and a_1 is normalized by dividing by 1000. This equation is plotted in Figure 14 for the case of a single reflection and $\theta = 10°$ in order to illustrate the general characteristics for $\delta = 0.01$. These results show that extremely high rates of acceleration or deceleration are required over the entire M_1 range if δ is as high as 0.01. For more reasonable accelerations, δ will be extremely small. It is apparent, that within this range of M_1, essentially steady state conditions exist during the deceleration or acceleration.

Equations (52) and (62), then, allow the computation of the pressure distribution along the decelerating or accelerating flat plate using a finite difference method. It has been shown that conditions during the change in velocities, for reasonable accelerations or decelerations, are essentially steady state. Thus, it is not felt by the

author that the problem of the deceleration or acceleration of a flat plate at hypersonic velocities is of great importance. It would appear, however, that the situation may be considerably different in the low supersonic regime.

It is felt that the problem of oscillating airfoils in the hypersonic velocity range could be of importance. As a side light to this investigation, therefore, the methods investigated above are applied to extend the theory of Lighthill (6) to include the effect of any number of reflections of the pressure disturbance wave. This extension is contained in the Appendix.

The methods outlined in this chapter apply only to Mach numbers in the hypersonic velocity range. It is seen that as supersonic velocities are approached, the piston theory results in errors of ten per cent or more. In the succeeding chapter, an approach is outlined for the supersonic case.

CHAPTER IV

SUPERSONIC CASE

The supersonic case is much more complex than the hypersonic case because, as explained earlier, the shock wave can not be assumed parallel to the flat plate surface, and the propagating and reflecting pressure disturbance waves can not be assumed parallel to each other. In fact, changes in the velocity tangential to the surface may become quite substantial in comparison with the changes normal to the surface. The theory of characteristics seems to provide the only method for accurately calculating the unsteady flow field behind a shock attached to a flat plate in supersonic flow. Since the author knows of no attempt to set up the theory of characteristics for this case, and since considerable effort was spent in studying this situation in an effort to understand the physical problem, some ideas and results will be presented herein.

Time would not allow a complete development of the theory of characteristics, although the most difficult analytical solution involving interactions at the shock wave is solved. In addition, the physical situation and remaining analytical developments, believed to be required for a solution, are established. In the subsequent paragraphs, the solution involving the interaction at the shock will first be developed. Then the physical wave situation existing between the shock wave and the flat plate surface will be discussed and a method for the solution of the wave motion in this area will be briefly outlined.

Shown in Figure 15 (a), is a flat plate at angle of attack θ, which has undergone an acceleration. For purposes of clarity, finite changes are illustrated and occasionally used in the derivation. At point A, a propagating wave, w_1, coalesces with the shock wave, s_1, causing a change in strength of the shock wave and a new pressure disturbance wave, w_2 to reflect. Also originating at this point because of the change in shock strength is an entropy interface shown by the dotted line.

Since point A is, and must remain, common to both shock s_1 and wave w_1, an equation may be written for the motion of point A along shock wave s_1. If this motion is denoted by dZ_A/dt, then

$$\frac{dZ_A}{dt} = \frac{C_{w_1}}{\sin(\beta - \theta)} - \frac{C_{s_1}}{\tan(\beta - \theta)} \tag{66}$$

In a similar manner, point A must remain common to both wave w_2 and shock s_1. For this case,

$$\frac{dZ_A}{dt} = \frac{C_{w_2}}{\sin \delta} + \frac{C_{s_1}}{\tan \delta} \tag{67}$$

Equating equations (66) and (67), and noting that in the limiting case, or case of small perturbations,

$$\frac{C_{w_1}}{a_1} = \left(\frac{a_2}{a_1}\right)_o + \frac{u_p}{a_1} \cos(\beta - \theta) \tag{68}$$

$$\frac{C_{s_1}}{a_1} = \frac{u_p}{a_1} \frac{\cos(\beta - \theta) \sin \beta}{\sin \theta} \tag{69}$$

and

$$\frac{C_{w_2}}{a_1} = \left(\frac{a_2}{a_1}\right)_o - \frac{u_p}{a_1} \text{ Cos } \delta \tag{70}$$

the following relationship for δ is obtained after some algebraic simplification.

$$\text{Sin } \delta = \frac{\left(\frac{a_2}{a_1}\right)_o X}{X^2 + Y^2} \pm \frac{Y}{X^2 + Y^2}\sqrt{X^2 + Y^2 - \left(\frac{a_2}{a_1}\right)_o^2} \tag{71}$$

where

$$X = \frac{\left(\frac{a_2}{a_1}\right)_o + M_1\left[\text{Sin } \theta - \text{Sin } \beta \text{ Cos } (\beta - \theta)\right]}{\text{Sin } (\beta - \theta)} \tag{72}$$

and

$$Y = M_1\left[\text{Sin } \beta - \frac{\text{Sin } \theta}{\text{Cos } (\beta - \theta)}\right] \tag{73}$$

In the same manner, a relation may be found between the angle $d\phi$ and C_{s2}. Considering wave w_1 and shock s_1, dZ_A/dt is again given by equation (66). The corresponding solution for shock s_2 and shock s_1 is

$$\frac{dZ_A}{dt} = \frac{C_{s1} + dC_s}{\text{Sin } d\phi} - \frac{C_{s1}}{\tan d\phi} \tag{74}$$

Setting equations (66) and (74) equal to each other and using the identities $\sin d\phi = \tan d\phi = d\phi$, the following relation is obtained.

$$\frac{dC_s}{a_1} = d\phi \left[G\right] \tag{75}$$

where

$$\left[G\right] = \frac{\left(\frac{a_2}{a_1}\right)_o + M_1 \text{ Sin } \theta}{(\text{Sin } (\beta - \theta)} - \frac{M_1 \text{ Sin } \beta}{\tan (\beta - \theta)} \tag{76}$$

A second expression involving dC_s is obtained from the shock relations from Liepmann and Roshko (8) given below.

$$\frac{C_s}{a_1} = \left(\frac{\gamma-1}{2\gamma} + \frac{\gamma+1}{2\gamma} \frac{p_2}{p_1}\right)^{1/2} \tag{77}$$

$$\frac{u_p}{a_1} = \frac{1}{\gamma} \left(\frac{p_2}{p_1} - 1\right)\left(\frac{\frac{2\gamma}{\gamma+1}}{\frac{p_2}{p_1} + \frac{\gamma-1}{\gamma+1}}\right)^{1/2} \tag{78}$$

Differentiating equations (77) and (78), gives

$$\frac{d \frac{C_s}{a_1}}{d \frac{p_2}{p_1}} = \frac{1}{2} \left(\frac{\gamma+1}{2\gamma}\right) \left[\frac{\frac{\gamma-1}{\gamma+1} + \left(\frac{p_2}{p_1}\right)_o}{\frac{2\gamma}{\gamma+1}}\right]^{-1/2} \tag{79}$$

$$\frac{d \frac{u_p}{a_1}}{d \frac{p_2}{p_1}} = \frac{1}{2\gamma} \left[\frac{\frac{2\gamma}{\gamma+1}}{\left(\frac{p_2}{p_1}\right)_o + \frac{\gamma-1}{\gamma+1}}\right]^{1/2} \left[\frac{\left(\frac{p_2}{p_1}\right)_o + \frac{3\gamma-1}{\gamma+1}}{\left(\frac{p_2}{p_1}\right)_o + \frac{\gamma-1}{\gamma+1}}\right] \tag{80}$$

From equations (79) and (80), it is found that

$$d\,\frac{C_s}{a_1} = \left[H\right]\; d\,\frac{u_p}{a_1} \tag{81}$$

where

$$\left[H\right] = \frac{\gamma+1}{2}\left[\frac{\left(\frac{p_2}{p_1}\right)_o + \frac{\gamma-1}{\gamma+1}}{\left(\frac{p_2}{p_1}\right)_o + \frac{3\gamma-1}{\gamma+1}}\right] \tag{82}$$

Substituting equation (81) into equation (75) gives

$$d\,\frac{u_p}{a_1} = d\phi\,\frac{\left[G\right]}{\left[H\right]} = d\phi\,\left[J\right] \tag{83}$$

which represents the change in flow velocity in area b of Figure 15 (a).

The angle ψ can also be determined by the compatibility condition at point A. The compatibility condition for the entropy interface and shock s_2 is

$$\tan\,(\delta - \psi) = \frac{C_{s2} - u_p}{\frac{dZ_A}{dt}} = \frac{C_{s1} - u_p}{\frac{C_{w1}}{\sin\,(\beta-\theta)} - \frac{C_{s1}}{\tan\,(\beta-\theta)}} \tag{84}$$

After simplifying, the relation for $\tan\,(\delta - \psi)$ is given by

$$\tan\,(\delta - \psi) = \frac{M_1\,\sin\,\beta - M_1\,\frac{\sin\,\theta}{\cos\,(\beta-\theta)}}{\frac{(a_2/a_1)_o + M_1\,\sin\,\theta}{\sin\,(\beta-\theta)} - \frac{M_1\,\sin\,\beta}{\tan\,(\beta-\theta)}} \tag{85}$$

The equations developed up to this point establish the wave geometry and a relationship between d C_s/a_1 and d u_p/a_1. Additional conditions are now required before either d C_s/a_1 and d u_p/a_1, and thus, the strength of wave w_2 can be determined.

First, wave w_2 is a plane wave which can only induce changes normal to the wave front. Thus, a required condition is that the tangential component of du across the wave w_2 must remain unchanged and equal to that in region d in Figure 15 (a). Second, the component of du normal to the entropy interface and the static pressure must be the same on both sides of the entropy interface.

The entropy interface will first be considered. Since flow slippage may occur at the entropy interface,

$$d\,\overline{\frac{u_{pa}}{a_1}} = d\,\overline{\frac{u_{pb}}{a_1}} + d\,\overline{\frac{u_{pat}}{a_1}} \tag{86}$$

where $\frac{du_{pat}}{a_1}$ is the change in slip velocity along the entropy interface. Let $(\ )_{\substack{nor\\w_2}}$ represent the component of velocity normal to wave w_2 and $(\ )_{\substack{tan\\w_2}}$ represent the component of change in velocity tangent to wave w_2. Then

$$\left(d\,\frac{u_{pa}}{a_1}\right)_{\substack{nor\\w_2}} = \left(d\,\frac{u_{pb}}{a_1}\right)_{\substack{nor\\w_2}} + \left(d\,\frac{u_{pat}}{a_1}\right)_{\substack{nor\\w_2}} \tag{87}$$

$$\left(d\,\frac{u_{pa}}{a_1}\right)_{\substack{tan\\w_2}} = \left(d\,\frac{u_{pb}}{a_1}\right)_{\substack{tan\\w_2}} + \left(d\,\frac{u_{pat}}{a_1}\right)_{\substack{tan\\w_2}} \tag{88}$$

From Figure 15 (a) it is seen that

$$\left(d\,\frac{u_{pb}}{a_1}\right)_{\substack{nor\\ w_2}} = \left(\frac{u_p}{a_1} + d\,\frac{u_{pb}}{a_1}\right)\,\mathrm{Cos}\,(\delta + d\phi) - \frac{u_p}{a_1}\,\cos\delta \tag{89}$$

$$\left(d\,\frac{u_{pb}}{a_1}\right)_{\substack{tan\\ w_2}} = \left(\frac{u_p}{a_1} + d\,\frac{u_{pb}}{a_1}\right)\,\mathrm{Sin}\,(\delta + d\phi) - \frac{u_p}{a_1}\,\sin\delta \tag{90}$$

After simplifying, eliminating second order terms, and substituting from equation (83) for $d\phi$, the following expressions are obtained.

$$\left(d\,\frac{u_{pb}}{a_1}\right)_{\substack{nor\\ w_2}} = \left[\mathrm{Cos}\,\delta - \frac{u_p}{a_1}\,\frac{\mathrm{Sin}\,\delta}{J}\right] d\,\frac{u_{pb}}{a_1} \tag{91}$$

$$\left(d\,\frac{u_{pb}}{a_1}\right)_{\substack{tan\\ w_2}} = \left[\mathrm{Sin}\,\delta + \frac{u_p}{a_1}\,\frac{\mathrm{Cos}\,\delta}{J}\right] d\,\frac{u_{pb}}{a_1} \tag{92}$$

Now noting that

$$\left(d\,\frac{u_{pat}}{a_1}\right)_{\substack{nor\\ w_2}} = -\left(d\,\frac{u_{pat}}{a_1}\right)\sin\psi \tag{93}$$

and

$$\left(d\,\frac{u_{pat}}{a_1}\right)_{\substack{tan\\ w_2}} = \left(d\,\frac{u_{pat}}{a_1}\right)\cos\psi \tag{94}$$

equations (87) and (88) become

$$\left(d\,\frac{u_{pa}}{a_1}\right)_{\substack{nor\\w_2}} = \left[\text{Cos}\ \delta - \frac{u_p}{a_1}\ \frac{\text{Sin}\ \delta}{J}\right]\ d\,\frac{u_{pb}}{a_1} - \left(d\,\frac{u_{pat}}{a_1}\right)\ \sin\psi \qquad (95)$$

$$\left(d\,\frac{u_{pa}}{a_1}\right)_{\substack{tan\\w_2}} = \left[\text{Sin}\ \delta + \frac{u_p}{a_1}\ \frac{\text{Cos}\ \delta}{J}\right] d\,\frac{u_{pb}}{a_1} + \left(d\,\frac{u_{pat}}{a_1}\right)\ \cos\psi \qquad (96)$$

Second, consider the changes across wave w_2. The component of change in velocity in area d, Figure 15 (a), tangent to wave w_2 is given in the limit by

$$\left(d\,\frac{u_p}{a_1}\right)_{\substack{tan\\w_2}} = d\,\frac{u_p}{a_1}\ \sin\,(\delta + \beta - \theta) \qquad (97)$$

Now, since $\left(d\,\frac{u_p}{a_1}\right)_{\substack{tan\\w_2}}$ is the same on both sides of wave w_2, equations (96) and (97) can be equated. Solving for $d\,\frac{u_{pat}}{a_1}$ gives,

$$d\,\frac{u_{pat}}{a_1} = \frac{1}{\text{Cos}\ \psi}\left[d\,\frac{u_p}{a_1}\ \sin\,(\delta + \beta - \theta) - d\,\frac{u_{pb}}{a_1}\,(\text{Sin}\ \delta + \frac{u_p}{a_1}\ \frac{\text{Cos}\ \delta}{J})\right] \qquad (98)$$

Now consider changes normal to wave w_2 for which the variable P would be constant. Holding P constant gives

$$\left[\frac{2}{\gamma-1}\ d\,\frac{a}{a_1} + \left(d\,\frac{u_p}{a_1}\right)_{\substack{nor\\w_2}}\right] = \left[\frac{2}{\gamma-1}\ d\,\frac{a_a}{a_1} + \left(d\,\frac{u_{pa}}{a_1}\right)_{\substack{nor\\w_2}}\right]_a \qquad (99)$$

The value of $\frac{2}{\gamma-1}\ d\ \frac{a_a}{a_1}$ can be obtained from the constant pressure condition that exists across the entropy interface

$$dS_b = \frac{2}{\gamma-1}\ \frac{d\ \frac{a}{a_1}}{\frac{a}{a_1}} = \frac{2}{\gamma-1}\ \frac{d\ \frac{a_b}{a_1} - d\ \frac{a_a}{a_1}}{\left(\frac{a_2}{a_1}\right)_o} \tag{100}$$

Substituting for dS_b from equation (36) and for $d\ a_b/a_1$ from equation (34), the following expression is obtained.

$$\frac{2}{\gamma-1}\ d\ \frac{a_a}{a_1} = \frac{\left(\frac{a_2}{a_1}\right)_o}{\gamma\ f_1\left(\frac{p_2}{p_1}\right)_o}\ d\ \frac{u_{pb}}{a_1} \tag{101}$$

In area d, the component of the change in piston velocity normal to wave w_2 is given by

$$\left(d\ \frac{u_p}{a_1}\right)_{\substack{nor\\ w_2}} = \left(d\ \frac{u_p}{a_1}\right) \text{Cos}\ (\delta + \beta - \theta) \tag{102}$$

If it is noted that across wave w_1, where the variable Q is a constant, that $\frac{2}{\gamma-1}\ d\ \frac{a}{a_1} = d\ \frac{u_p}{a_1}$ and if equations (95), (101), and (102) are substituted into equation (99), a second equation for $d\ \frac{u_{pat}}{a_1}$ is obtained giving

$$d\,\frac{u_{pat}}{a_1} = \frac{1}{\operatorname{Sin}\psi}\left\{\left[\frac{\left(\frac{a_2}{a_1}\right)_o}{\gamma\, f_1\left(\frac{p_2}{p_1}\right)_o} + \operatorname{Cos}\delta - \frac{u_p}{a_1}\,\frac{\operatorname{Sin}\delta}{J}\right] d\,\frac{u_{pb}}{a_1} - \left[1 + \operatorname{Cos}(\delta + \beta - \theta)\right] d\,\frac{u_p}{a_1}\right\} \tag{103}$$

Equation (103) can then be set equal to equation (98) and the following expression for $d\,\frac{u_{pb}}{a_1}$ obtained.

$$d\,\frac{u_{pb}}{a_1} = \left[K\right] d\,\frac{u_p}{a_1} \tag{104}$$

where

$$K = \frac{1 + \operatorname{Cos}(\delta + \beta - \theta) + \operatorname{Sin}(\delta + \beta - \theta)\tan\psi}{\frac{\left(\frac{a_2}{a_1}\right)_o}{\gamma\, f_1\left(\frac{p_2}{p_1}\right)_o} + \operatorname{Cos}\delta - \frac{u_p}{a_1}\,\frac{\operatorname{Sin}\delta}{J} + \left(\operatorname{Sin}\delta + \frac{u_p}{a_1}\,\frac{\operatorname{Cos}\delta}{J}\right)\tan\psi} \tag{105}$$

Introducing equation (104) into equation (98),

$$d\,\frac{u_{pat}}{a_1} = \frac{1}{\operatorname{Cos}\psi}\left[\operatorname{Sin}(\delta + \beta - \theta) - K\left(\operatorname{Sin}\delta + \frac{u_p}{a_1}\,\frac{\operatorname{Cos}\delta}{J}\right)\right] d\,\frac{u_p}{a_1} \tag{106}$$

Then substituting equations (104) and (106) into equation (95) gives

$$\left(d\,\frac{u_{pa}}{a_1}\right)_{\substack{nor\\ w_2}} = d\,\frac{u_p}{a_1}\left\{K\left(\operatorname{Cos}\delta - \frac{u_p}{a_1}\,\frac{\operatorname{Sin}\delta}{J}\right) - \tan\psi \left[\sin(\delta + \beta - \theta) - K\left(\operatorname{Sin}\delta + \frac{u_p}{a_1}\,\frac{\operatorname{Cos}\delta}{J}\right)\right]\right\} \tag{107}$$

Finally, since

$$(dQ)_{\substack{nor \\ w_2}} = \frac{2}{\gamma-1} \; d \frac{a_a}{a_1} - \left(d \frac{u_{pa}}{a_1}\right)_{\substack{nor \\ w_2}} \tag{108}$$

equations (101), (104) and (107) may be substituted into equation (108). Recognizing that $dP = 2\, du_p/a_1$, the following expression results

$$(dQ)_{\substack{nor \\ w_2}} = \frac{dP}{2}\left\{ \frac{\left(\frac{a_2}{a_1}\right)_o}{\gamma\, f_1\left(\frac{p_2}{p_1}\right)_o} K - K\left(\cos\delta - \frac{u_p}{a_1}\,\frac{\sin\delta}{J}\right) + \right. \tag{109}$$

$$\left. \tan\psi\left[\sin(\delta + \beta - \theta) - K\left(\sin\delta + \frac{u_p}{a_1}\,\frac{\cos\delta}{J}\right)\right]\right\}$$

It is interesting to note that in the limit when $\delta = \psi = (\beta - \theta) = 0$, the above expression for $(dQ)_{\substack{nor \\ w_2}}$ reduces to the same expression as derived for the hypersonic case. This is, of course, a necessary condition. Equation (107) or (109) expresses the strength of the reflected wave in terms of initial conditions. K, δ, J, and ψ, are all explicitly defined by initial conditions.

The equations outlined above, are valid for the matching of conditions at a point on the shock wave where a propagating wave, a reflected wave and an entropy interface meet. Also, the equations can immediately be applied in a finite difference solution. For M = 2.0, it is found that $\delta = 134.6°$ and $\psi = 81.95°$. If M were decreased further, δ would become larger, whereas, if M were increased, δ would become smaller until in the hypersonic case, δ would become approximately zero.

To carry the solution further, the reflected wave at point A must be a continuous part of the wave front which originated at the nose of the flat plate at the time of the change in velocity and traveled downstream along the plate surface to point D in Figure 15 (b). That is, the wave generated at the tip of the flat plate at time $t = 0$ has grown and moved downstream and is now a part of the same wave which is reflected at point A at some time later. This entire wave network grows continuously with time, maintaining similarity. It is possible to calculate the distance along the flat plate which the wave, generated at $t = 0$, has traveled. Rough scaling for the case $M = 2.0$, indicates that the reflected wave from point A must curve toward the nose of the flat plate as it travels toward the flat plate, in order for there to be compatibility at the plate surface. That this must be true is also seen from the fact that if the reflected wave from point A were allowed to strike the flat plate at an angle greater than 90°, measured clockwise from the flat plate surface, there would be no reflected wave solution which would keep the point of incidence and reflection in contact with the flat plate as the flat plate moves through the air.

The equations necessary to establish compatibility at the shock wave are now known and the condition for compatibility at the flat plate surface has been discussed. Conclusions made thus far indicate that the reflected wave from the shock wave to the flat plate surface is curved in order to satisfy compatibility requirements at both end points. It remains to discuss a method by which the wave pattern between the flat plate and shock wave may be determined.

It may be postulated that in the case of the infinite flat plate, just as in the case of the infinite cone, there is no scale factor and, that between the flat plate and shock, similarity must exist along radial lines, originating at the nose of the flat plate. The area between the flat plate and shock may then be divided into a finite number of areas by radial lines as indicated in Figure 15 (b). The strength and direction of travel of wave w_2 are known at point A and these same values may be assumed to exist at point B, similar to the case of steady flow characteristics. Wave w_3, propagating into area 2, joins with wave w_2 at point B.

Now the similarity condition demands that the wave pattern grows with time such that B moves to B', A moves to A', D moves to D', etc., expanding but maintaining similarity. This change with time is illustrated in Figure 15 (b). Thus, the compatibility condition at point B establishes the direction of wave w_3. Furthermore, a third wave, w_4, must intersect point B such that conditions in region 4 as obtained by the flow passing through waves w_2 and w_4 in series, are the same as those obtained by the flow passing through wave w_3. The direction of w_4 is again established by the compatibility condition at point B. With the direction of waves w_3 and w_4 established, only one solution of the plane wave equation exists for the strength of w_3 and w_4.

Wave w_3 will then be known after the above solution at point B is known. The same process may be repeated at point C and the reflected wave carried on, step-by-step, to the flat plate surface. At the surface, the boundary condition dictates that the only component of flow velocity must be the component tangent to the surface. The solutions

at points B, C, etc., may also be iterated as in standard steady state characteristic solutions.

At the same time, wave w_4 is known from the solution at point B. The solution for wave w_4 across the entropy interface may be found from equations previously developed and the intersection of wave w_4 with the shock wave at point E may be determined. The equations developed in the first part of this chapter may again be used to find a solution at point E which is compatible with existing conditions.

By following a step-by-step procedure similar to that outlined above, the entire wave pattern in the area between the flat plate and shock wave may be determined, and the pressure distribution calculated. The solution of a sample problem is left to later investigations.

CHAPTER V

CONCLUSIONS

Piston theory, incorporating the theory of characteristics and considering the entropy gradient across the attached shock, has been used to obtain a numerical-graphical and an analytic solution which give good results to the problem of pressure distribution along an accelerating flat plate at an angle of attack in the hypersonic velocity regime. For $\gamma = 1.4$ it was shown that:

(1) The hypersonic solution developed herein is good to within an accuracy of one per cent for values of Mach number greater than 5.6,

(2) a modified piston theory could be used which gave accuracies within one per cent down to a Mach number of 4.0,

(3) the so-called shock expansion theory solution to the problem contains considerable error,

(4) the first reflection of disturbance waves from the shock wave accounts for the major correction of the pressure back toward steady state value,

(5) the second reflection also contributes a non-negligible correction but higher order reflections may be disregarded,

(6) the reflection time for a disturbance wave is so short that for normal accelerations, the problem may be considered as essentially a steady state problem, and

(7) the hypersonic theory developed is directly applicable to the case of oscillating flat plates and can be used to extend the theory of

Lighthill (6). A sample extension is illustrated in the Appendix.

In the supersonic case, the piston theory method resulted in poor accuracy because of the effect of changes in the velocity component tangent to the plate surface. It was shown that the theory of characteristics could be developed for a complete step-by-step solution to the supersonic case. Equations were developed for the most difficult problem, that of matching conditions at the shock wave. In addition, a discussion was presented concerning the disturbance wave network existing between the flat plate and the shock wave, and a step-by-step solution for this network and the resulting pressure distribution was outlined. A complete solution of an example problem was left to later investigations.

A P P E N D I X

APPENDIX

EXTENSION OF THE METHOD OF LIGHTHILL

In reference (6), Lighthill uses piston theory to determine the pressure distribution on an oscillating airfoil at high Mach numbers. Essentially, use is made of the first three terms of the binomial expansion of the "simple wave" condition

$$\frac{p}{p_1} = \left(1 + \frac{\gamma-1}{2} \frac{u}{a_1}\right)^{\frac{2\gamma}{\gamma+1}} \tag{110}$$

where u/a_1 is the perturbation velocity of the airfoil normal to the stream. Thus, no reflections of the pressure disturbance wave are considered in the solution.

As a result of the work presented in Chapter III, Lighthill's results can now be extended to account for the pressure change resulting from wave reflections from the shock wave for the flat plate case. The value of the ratio a/a_1 will be determined as a function of time on the flat plate surface. Since the entropy is constant in the area of the flat plate surface, the isentropic relation, equation (24), may be used to give the pressure at any time t.

Initially it is known that along the flat plate surface

$$Q = \frac{2}{\gamma-1} \frac{a}{a_1} - \frac{u}{a_1} \tag{111}$$

and

$$P = \frac{2}{\gamma-1}\,\frac{a}{a_1} + \frac{u}{a_1} \tag{112}$$

Differentiating with respect to time,

$$\frac{dQ}{dt} = \frac{2}{\gamma-1}\,\frac{d\,\frac{a}{a_1}}{dt} - \frac{d\,\frac{u}{a_1}}{dt} \tag{113}$$

and

$$\frac{dP}{dt} = \frac{2}{\gamma-1}\,\frac{d\,\frac{a}{a_1}}{dt} + \frac{d\,\frac{u}{a_1}}{dt} \tag{114}$$

From equation (47),

$$\frac{dQ(t)}{dt} = \left[F\right]\,\frac{dP(t-\eta)}{dt} \tag{115}$$

where η is the time required for the reflection of a disturbance wave. Substituting from equations (113) and (114),

$$\frac{2}{\gamma-1}\,\frac{d\,\frac{a}{a_1}(t)}{dt} - \frac{d\,\frac{u}{a_1}(t)}{dt} = \left(F\right)\left[\frac{2}{\gamma-1}\,\frac{d\,\frac{a}{a_1}(t-\eta)}{dt} + \frac{d\,\frac{u}{a_1}(t-\eta)}{dt}\right] \tag{116}$$

If the flat plate is assumed to have a velocity normal to the free stream

$$\frac{u}{a_1}(t) = \frac{\overline{u}}{a_1} + A \sin 2\pi f t \tag{117}$$

where A is the maximum perturbation amplitude and $\overline{u/a_1}$ is the steady state velocity, the velocity may be differentiated with respect to time yielding,

$$\frac{d\,\frac{u}{a_1}(t)}{dt} = 2\pi f\ A\ \mathrm{Cos}\ 2\pi ft \tag{118}$$

and

$$\frac{d\,\frac{u}{a_1}(t-\eta)}{dt} = 2\pi f\ A\ \mathrm{Cos}\ 2\pi f\ (t-\eta) \tag{119}$$

Substituting equations (118) and (119) into equation (116) and rearranging,

$$\frac{2}{\gamma-1}\left[\frac{d\,\frac{a}{a_1}(t)}{dt} - F\,\frac{d\,\frac{a}{a_1}(t-\eta)}{dt}\right] = 2\pi f\ A\ \mathrm{Cos}\ 2\pi ft + 2\pi fAF\ \mathrm{Cos}\ 2\pi f(t-\eta) \tag{120}$$

If F is zero, Lighthill's solution is obtained, that is

$$\frac{a}{a_1}(t) = \frac{\gamma-1}{2}\left(\mathrm{Sin}\ 2\pi ft + C\right) \tag{121}$$

or

$$\frac{a}{a_1}(t) = \left(\frac{a_2}{a_1}\right)_o + \left(\frac{\gamma-1}{2}\right) A\ \mathrm{Sin}\ 2\pi ft \tag{122}$$

where the boundary condition used is that at $t = 0$, $a/a_1 = (a_2/a_1)_o$.

If F is small and assumed constant, that is, if the velocity changes are small, a solution of the following form may be assumed.

$$\frac{a}{a_1}(t) = \frac{\gamma-1}{2}\left[A\ \sin 2\pi ft + F\ f_1(t) + F^2\ f_2(t) + \ldots + F^n f_n(t)\right] \tag{123}$$

where n in this case would represent the number of reflections. By differentiating the assumed solution with respect to time and substituting into equation (120), expressions may be obtained for the functions $f_1'(t)$, $f_2'(t)$, ..., $f_n'(t)$. Performing this operation and substituting into the differential equation obtained from differentiating the assumed solution for $a/a_1(t)$ with respect to time, it is found that

$$\frac{d\,\frac{a}{a_1}(t)}{dt} = \frac{\gamma-1}{2}\Big[2\pi fA \operatorname{Cos} 2\pi ft + F4\pi\, fA \operatorname{Cos} 2\pi f\,(t-\eta) + F^2\, 4\pi f\, A \operatorname{Cos} 2\pi f(t-2\eta) + \ldots + F^n 4\pi fA \operatorname{Cos} 2\pi f(t-n\eta)\Big] \tag{124}$$

Equation (120) is a linear differential equation. The solution of equation (120), however, differs from the solution of a standard differential equation in that boundary conditions must be specified over a finite interval of time. As a typical example of a solution, it is assumed that the oscillating motion has been going on for an indefinite period of time, and that at $t = 0$, $a/a_1 = (a_2/a_1)_o$. Equation (124) may then be integrated to obtain the solution for $a/a_1\ (t)$ as follows.

$$\frac{a}{a_1}(t) = \left(\frac{a_2}{a_1}\right)_o + \frac{\gamma-1}{2} A\Big\{ \operatorname{Sin} 2\pi ft + F\Big[\operatorname{Sin} 2\pi f(t-\eta) + \operatorname{Sin} 2\pi f\eta\Big] + F^2\Big[\operatorname{Sin} 2\pi f(t-2\eta) + \operatorname{Sin} 4\pi f\eta\Big] + \ldots + F^n\Big[\operatorname{Sin} 2\pi f(t-n\eta) + \operatorname{Sin} 2n\pi f\eta\Big]\Big\} \tag{125}$$

The pressure may be obtained at any time t, then, by the expression

$$\frac{p}{p_1} = \left[\frac{a}{a_1}(t)\right]^{\frac{2\gamma}{\gamma-1}} \tag{126}$$

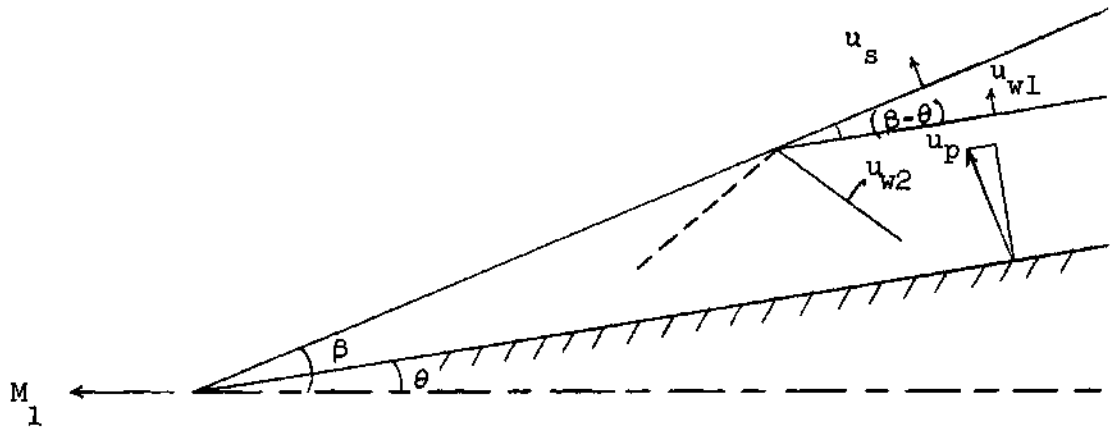

a) Supersonic Case

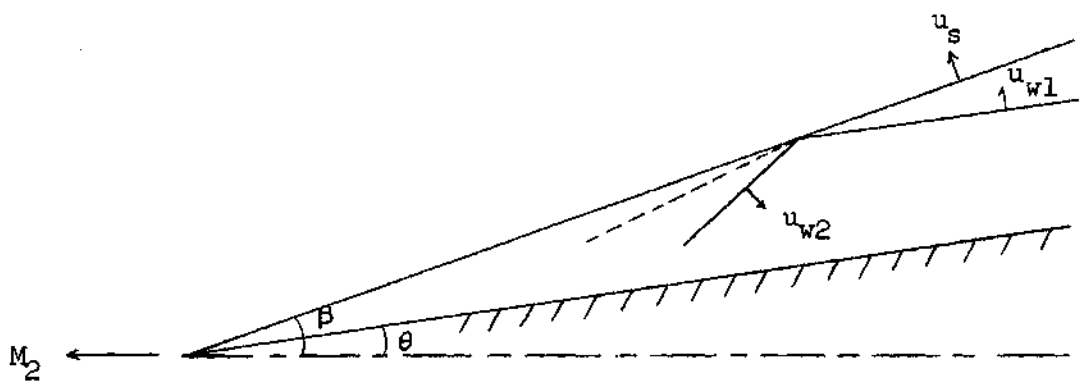

b) High Supersonic Case, $M_2 > M_1$

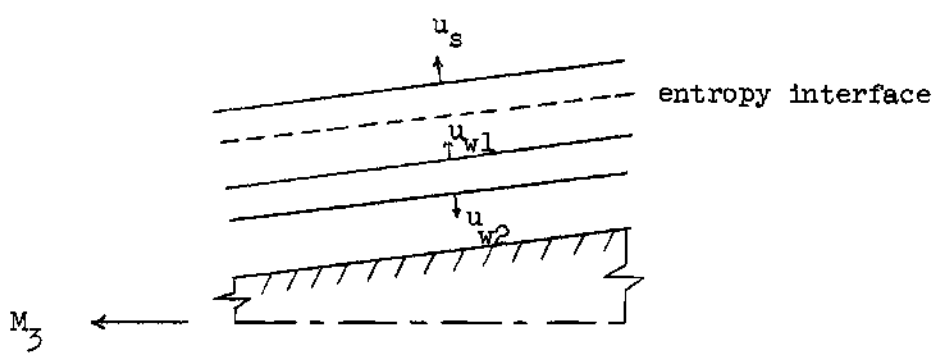

c) Hypersonic Case $M_3 \gg M_1$

Figure 1. The Physical Problem.

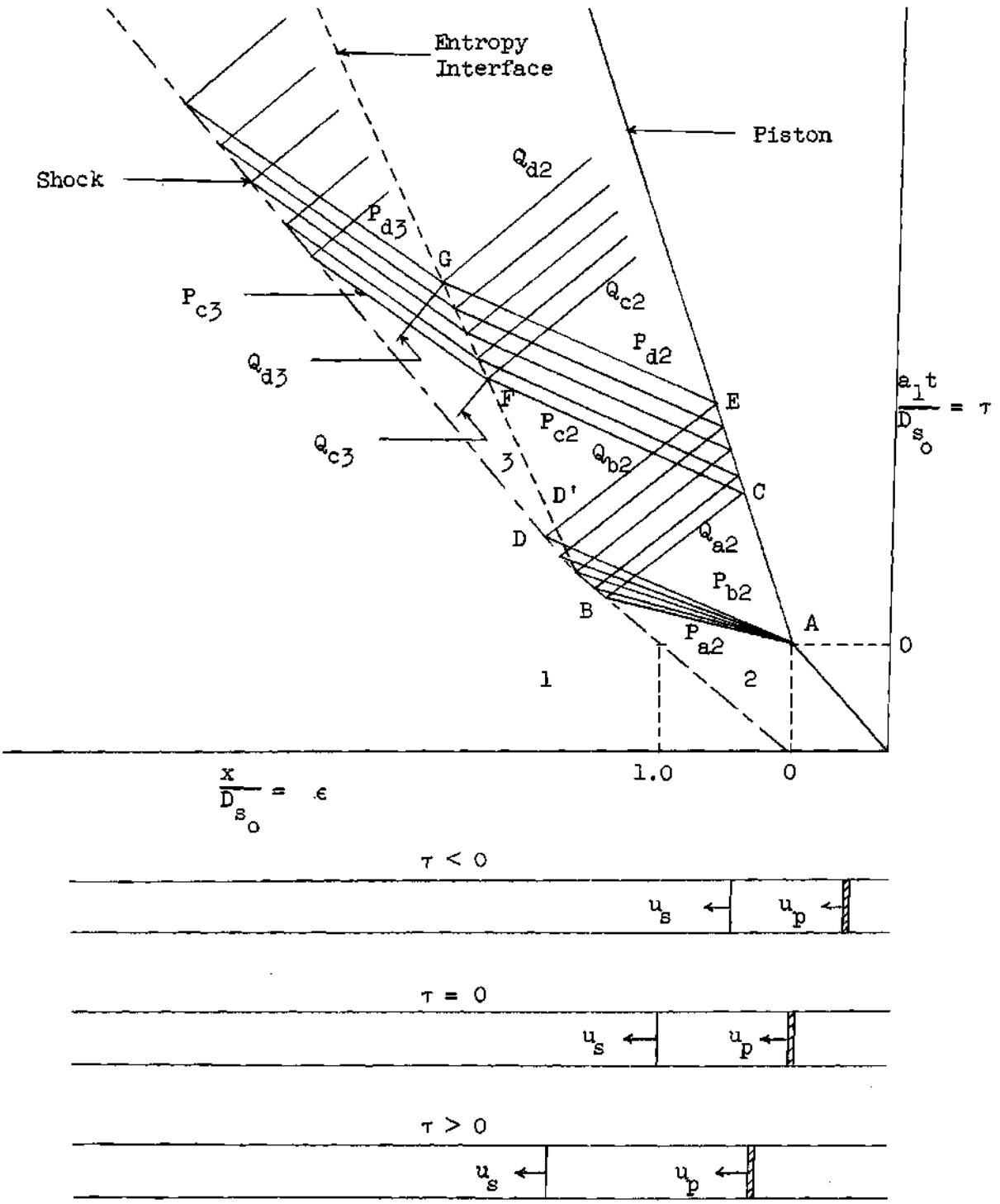

Figure 2. Numerical Integration of Wave Equations in ϵ - τ plane for a Sudden Decrease in Piston Velocity.

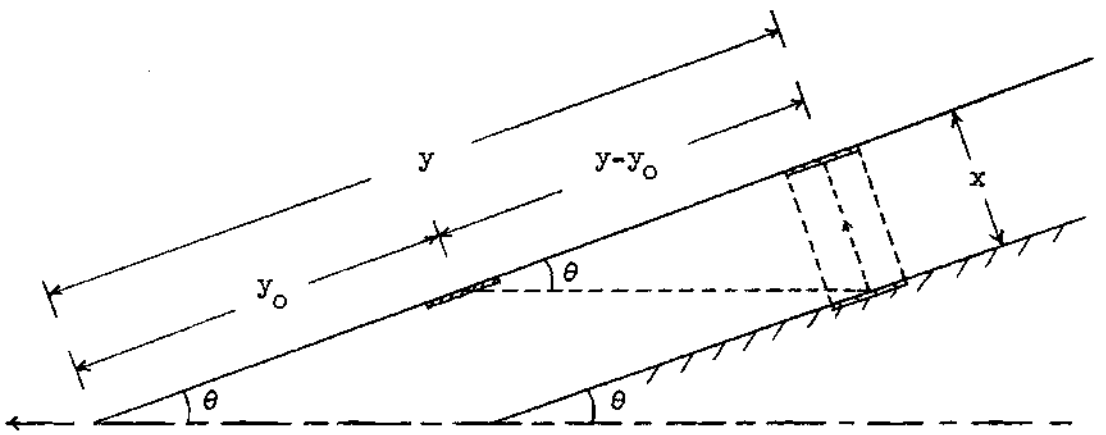

(a)

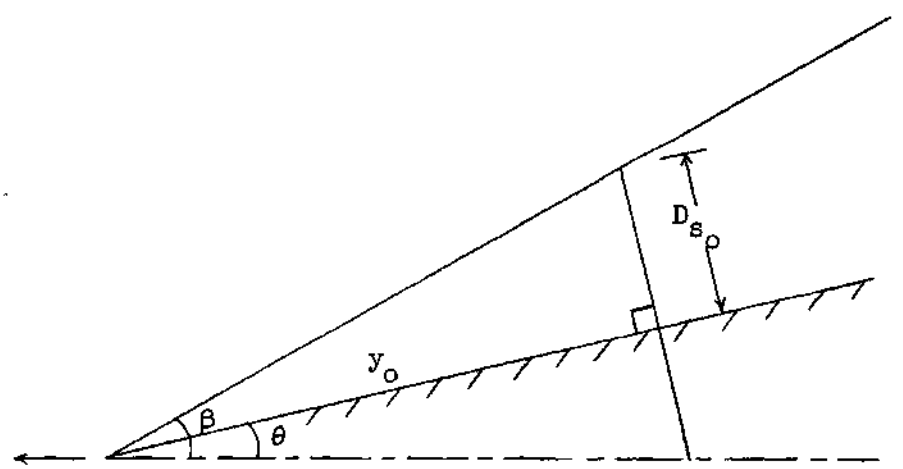

(b)

Figure 3. Relation between x, y, D_{s_o}, β and θ for Flat Plate.

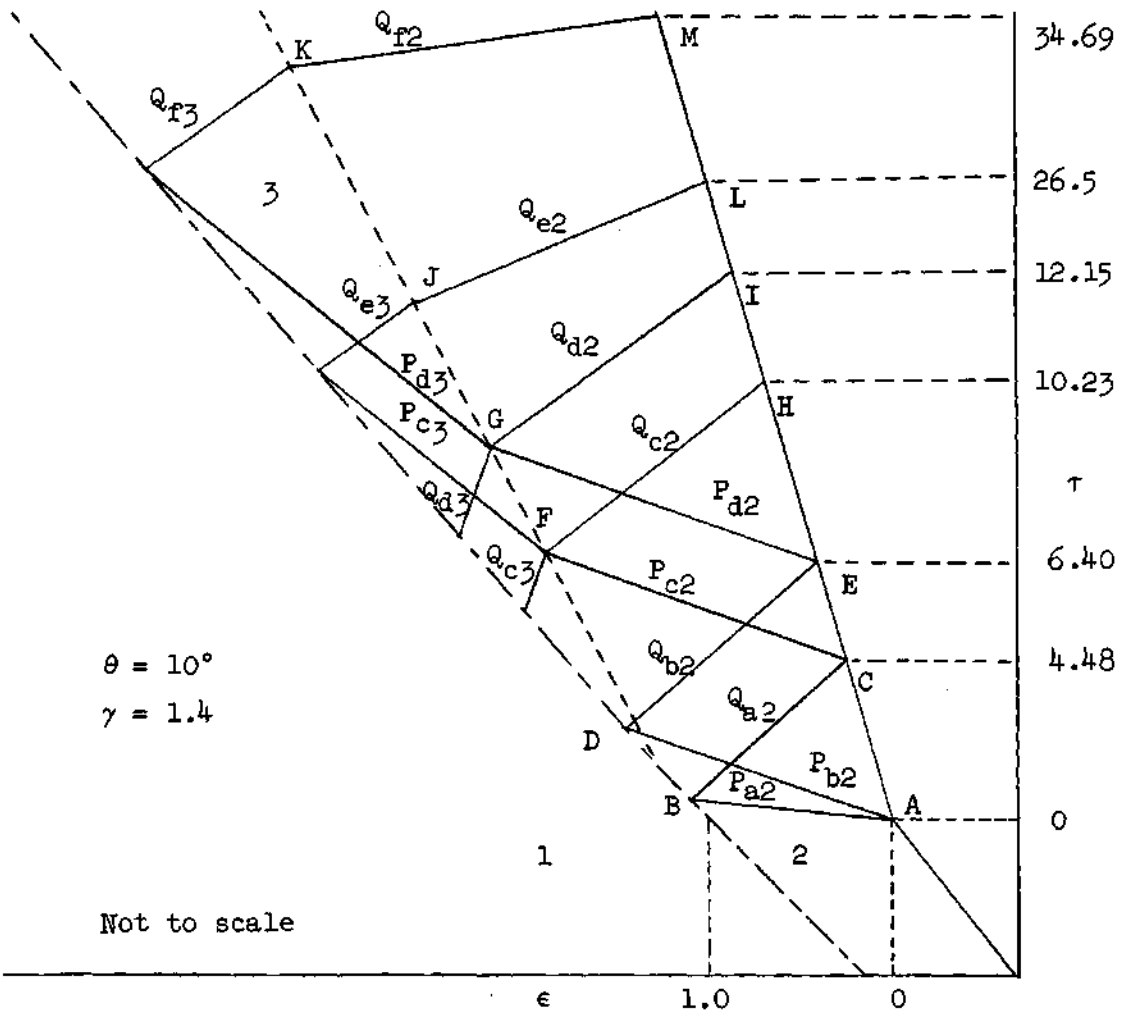

P_{a2} = 7.246635	Q_{c2} = 5.161416	A_A initial = 1.2392
P_{b2} = 6.904943	Q_{d2} = 5.161506	A_A final = 1.205031
P_{c2} = 6.904943	Q_{e2} = 5.161506	A_C = 1.205031
P_{d2} = 6.920994	Q_{f2} = 5.163666	A_E = 1.208241
P_{c3} = 6.840054	Q_{c3} = 5.095946	A_H = 1.208241
P_{d3} = 6.855439	Q_{d3} = 5.095946	A_I = 1.208259
Q_{a2} = 5.145365	Q_{e3} = 5.095946	A_L = 1.208259
Q_{b2} = 5.161416	Q_{f3} = 5.098102	A_M = 1.208691

Figure 4. ε-τ Plane for Step Deceleration of Flat Plate From M = 6.0 to M = 5.0.

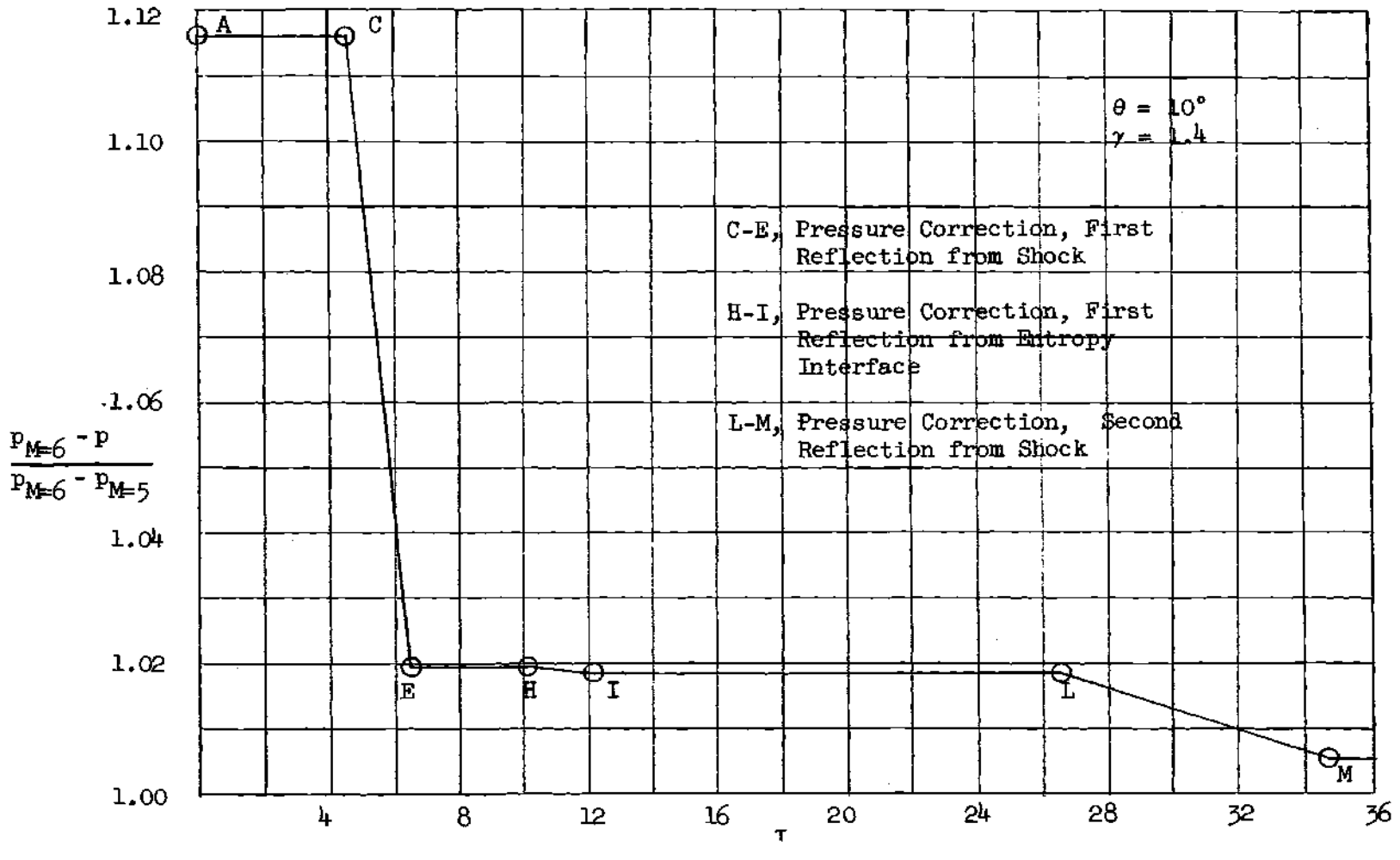

Figure 5. Pressure versus τ for Step Deceleration of Flat Plate From M = 6.0 to M = 5.0.

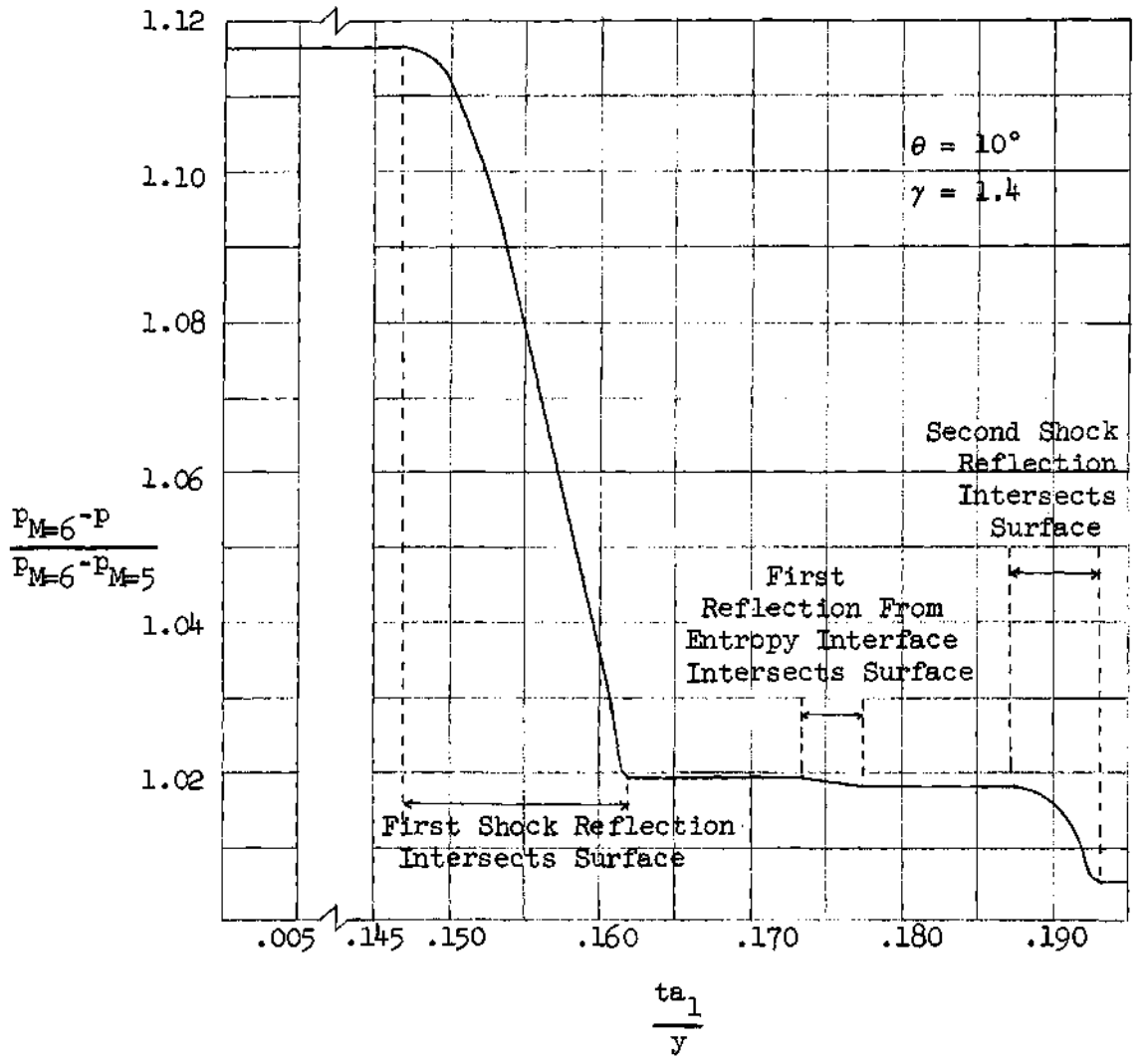

Figure 6. Pressure versus Time and Distance for Step Deceleration of Flat Plate from M = 6.0 to M = 5.0.

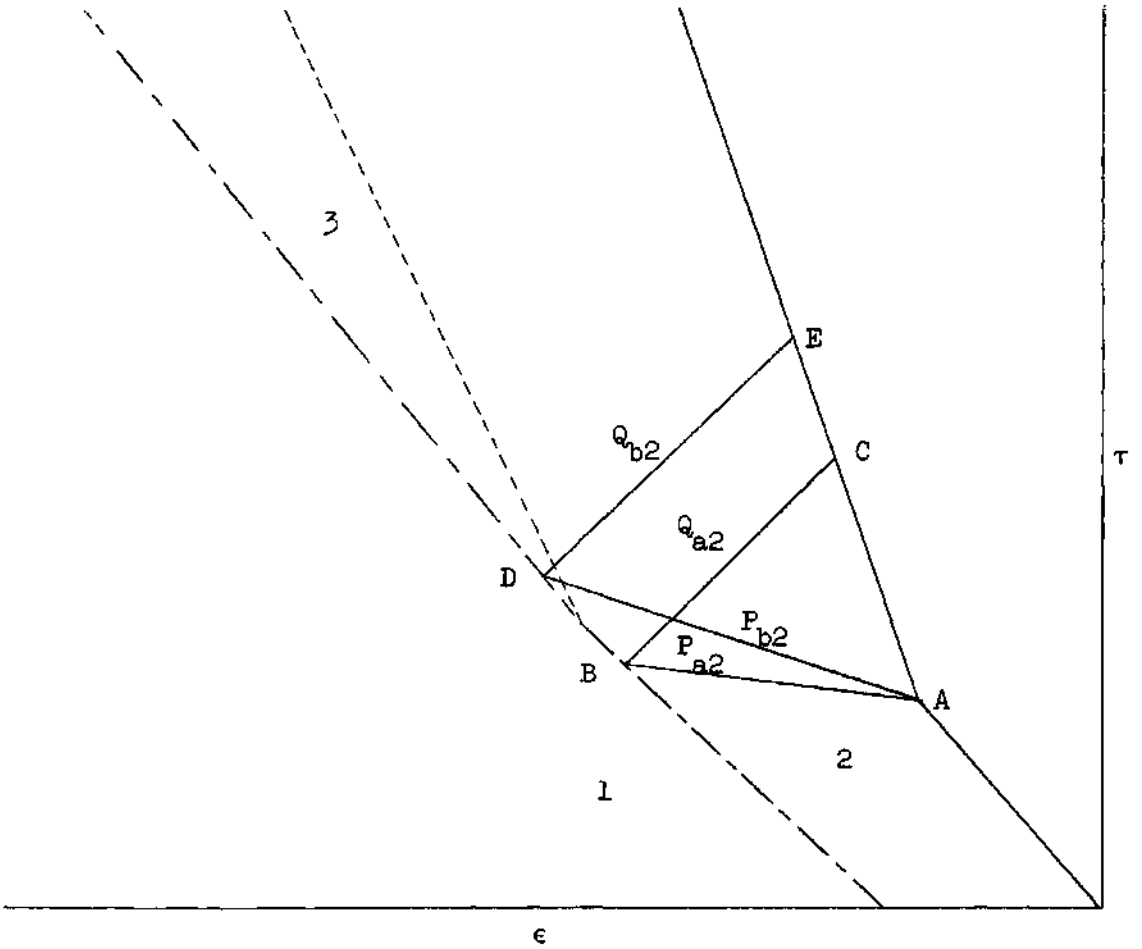

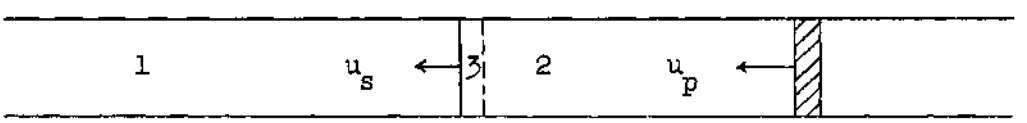

Figure 7. ϵ-τ Plane for Development of Analytic Solution

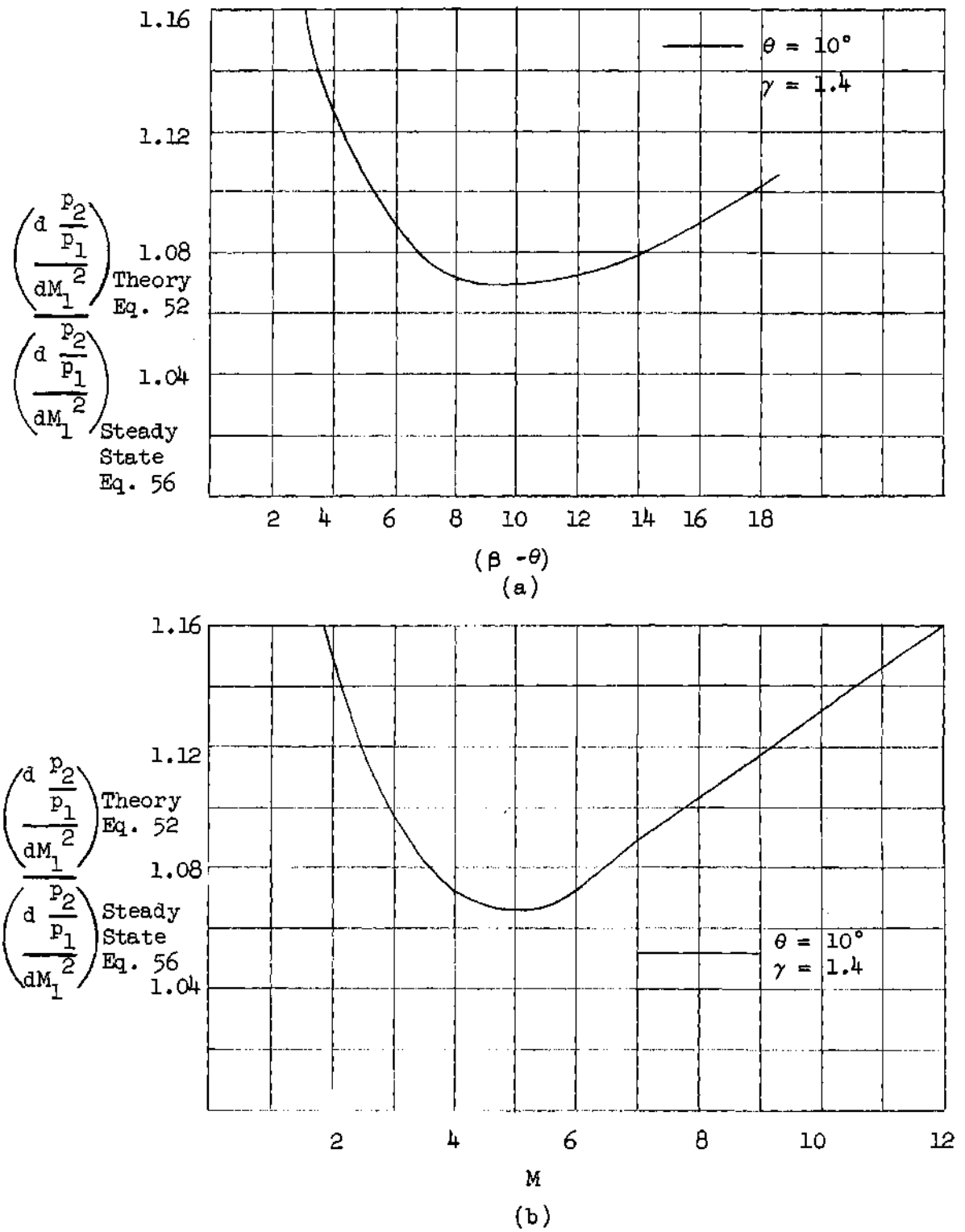

Figure 8. Pressure versus M and $(\beta - \theta)$ For No Reflections.

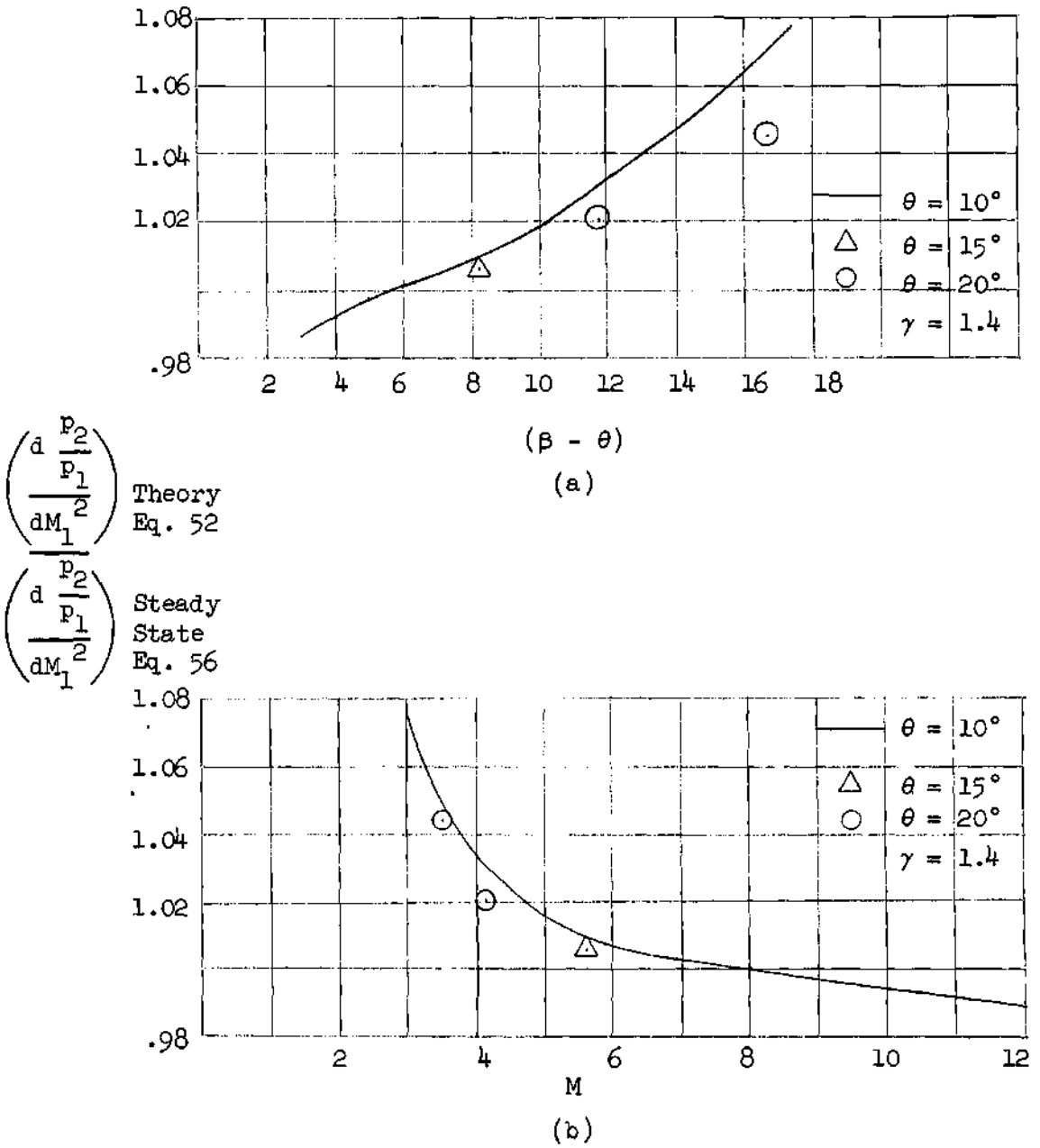

Figure 9. Pressure versus M and $(\beta - \theta)$ For One Reflection

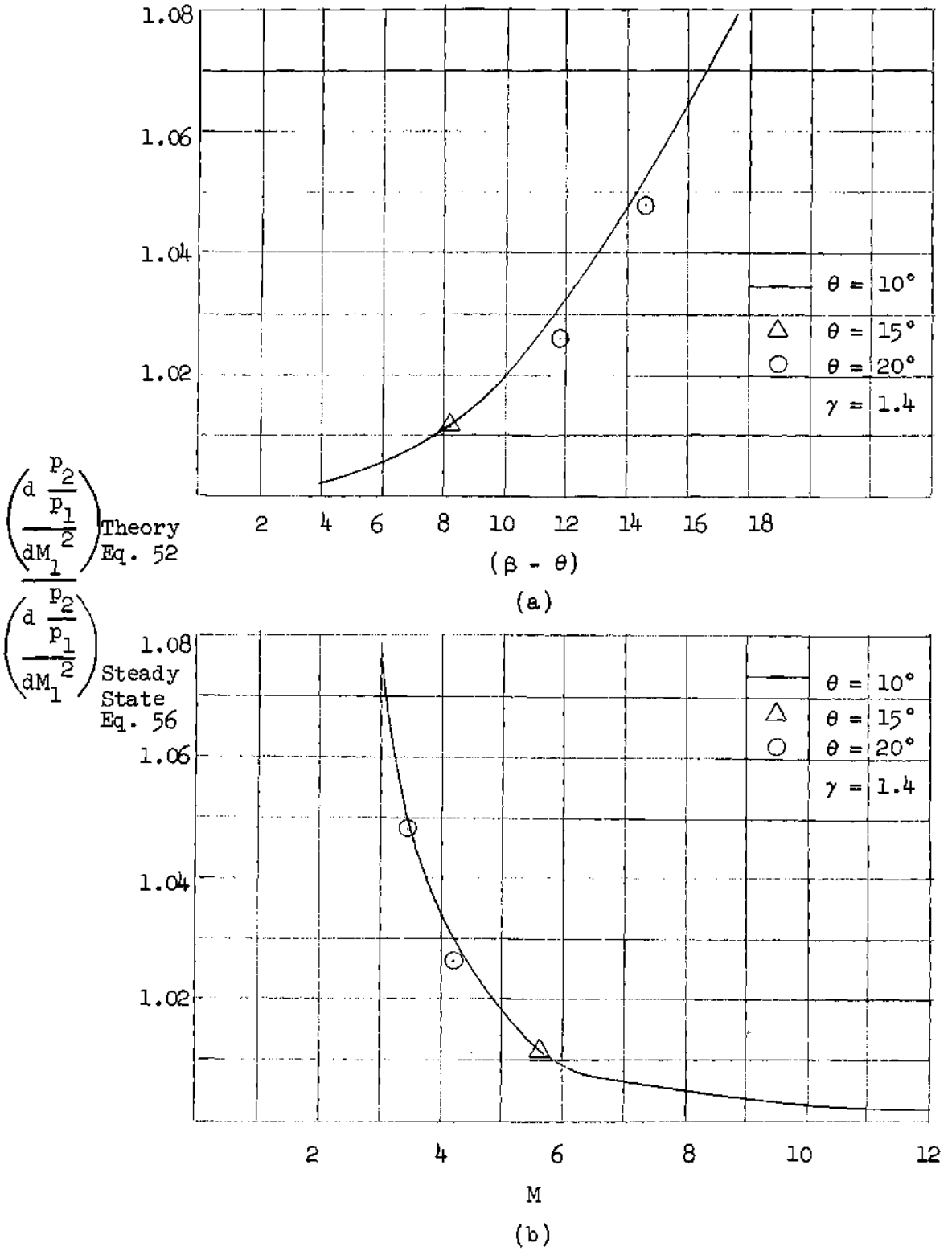

Figure 10. Pressure versus M and $(\beta - \theta)$ For Two Reflections.

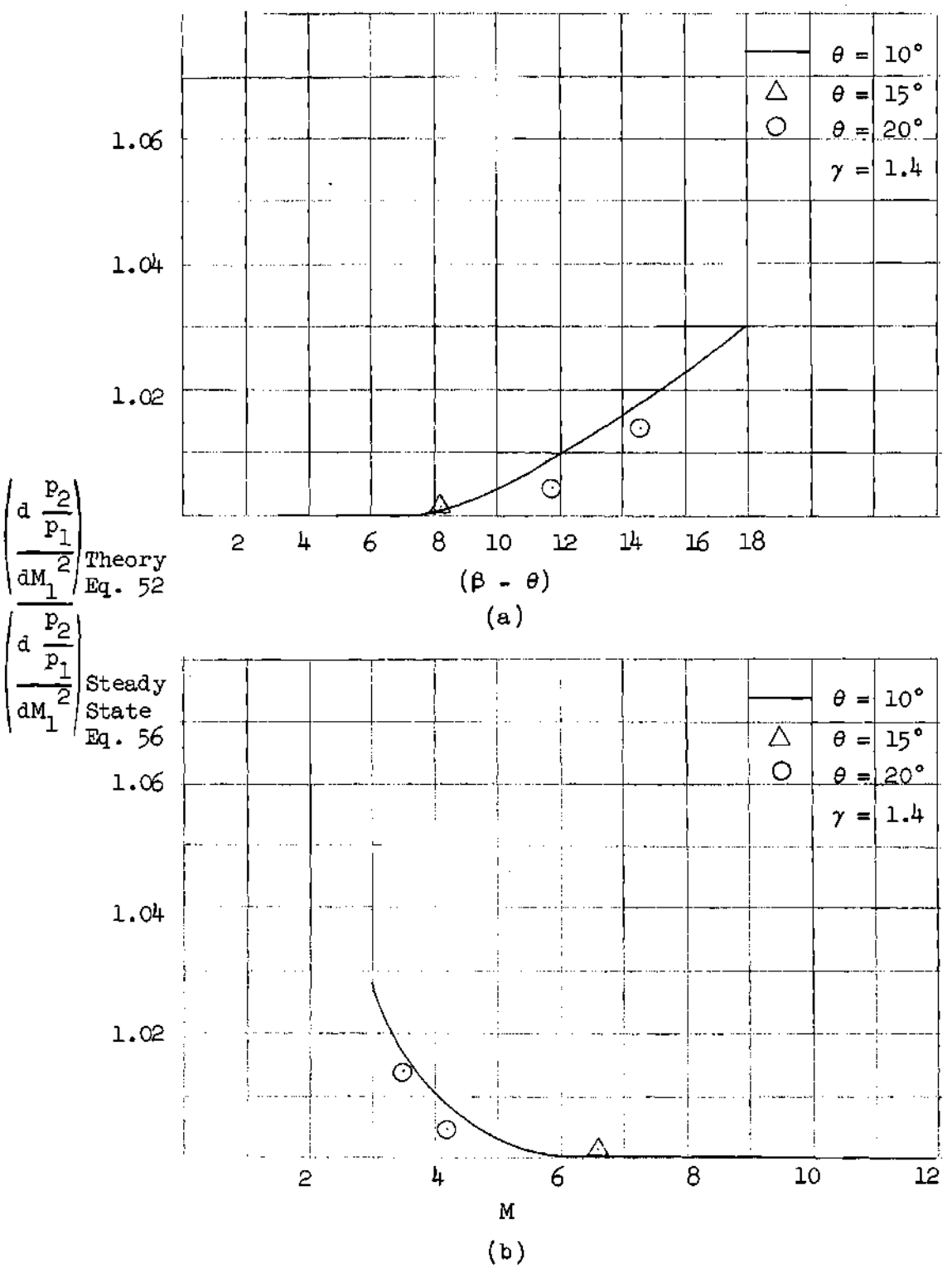

Figure 11. Pressure versus M and (β - θ) for Two Reflections with Modified piston Theory

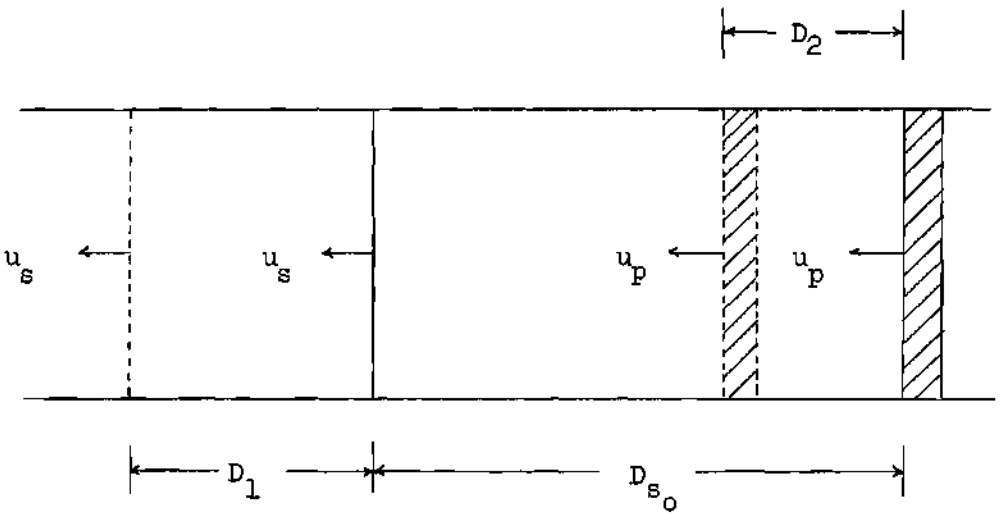

Figure 12. Relation Between Piston, Shock and Disturbance Wave for Determination of Time Lapse.

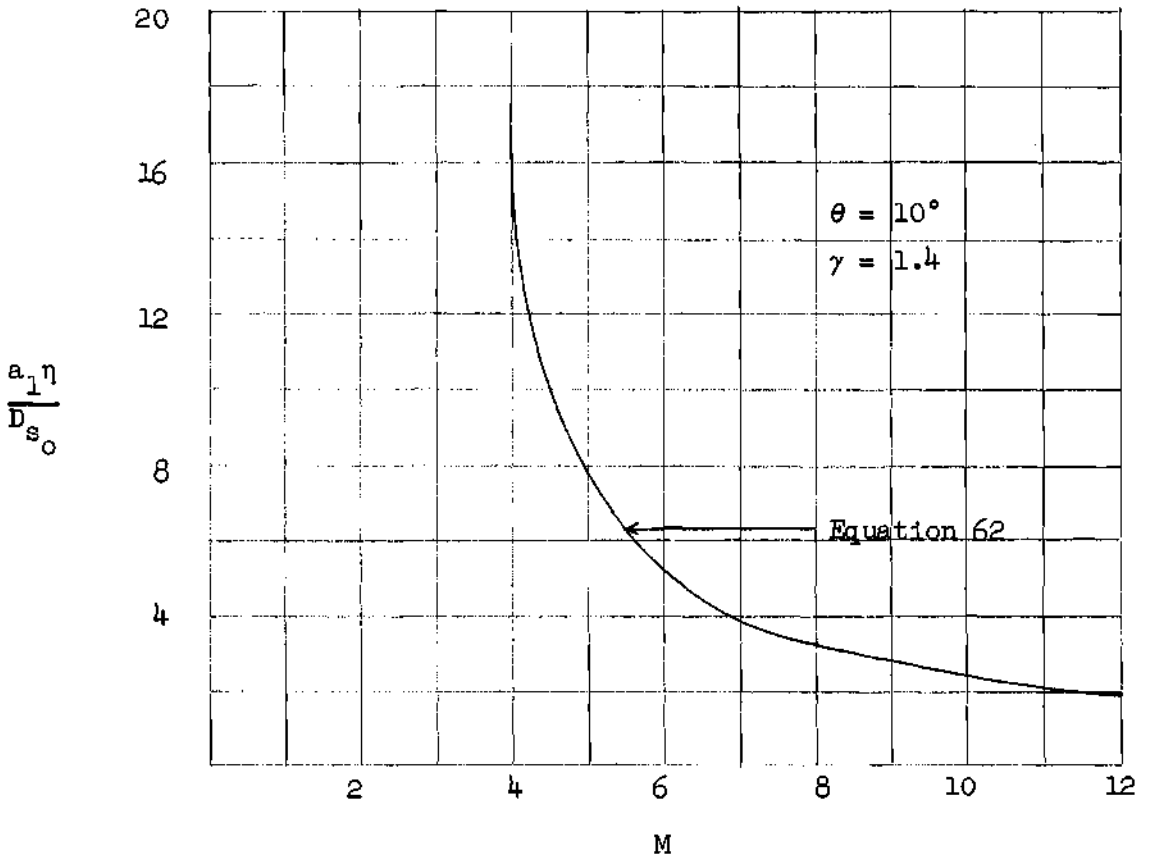

Figure 13. Time for One Reflection Versus Mach Number.

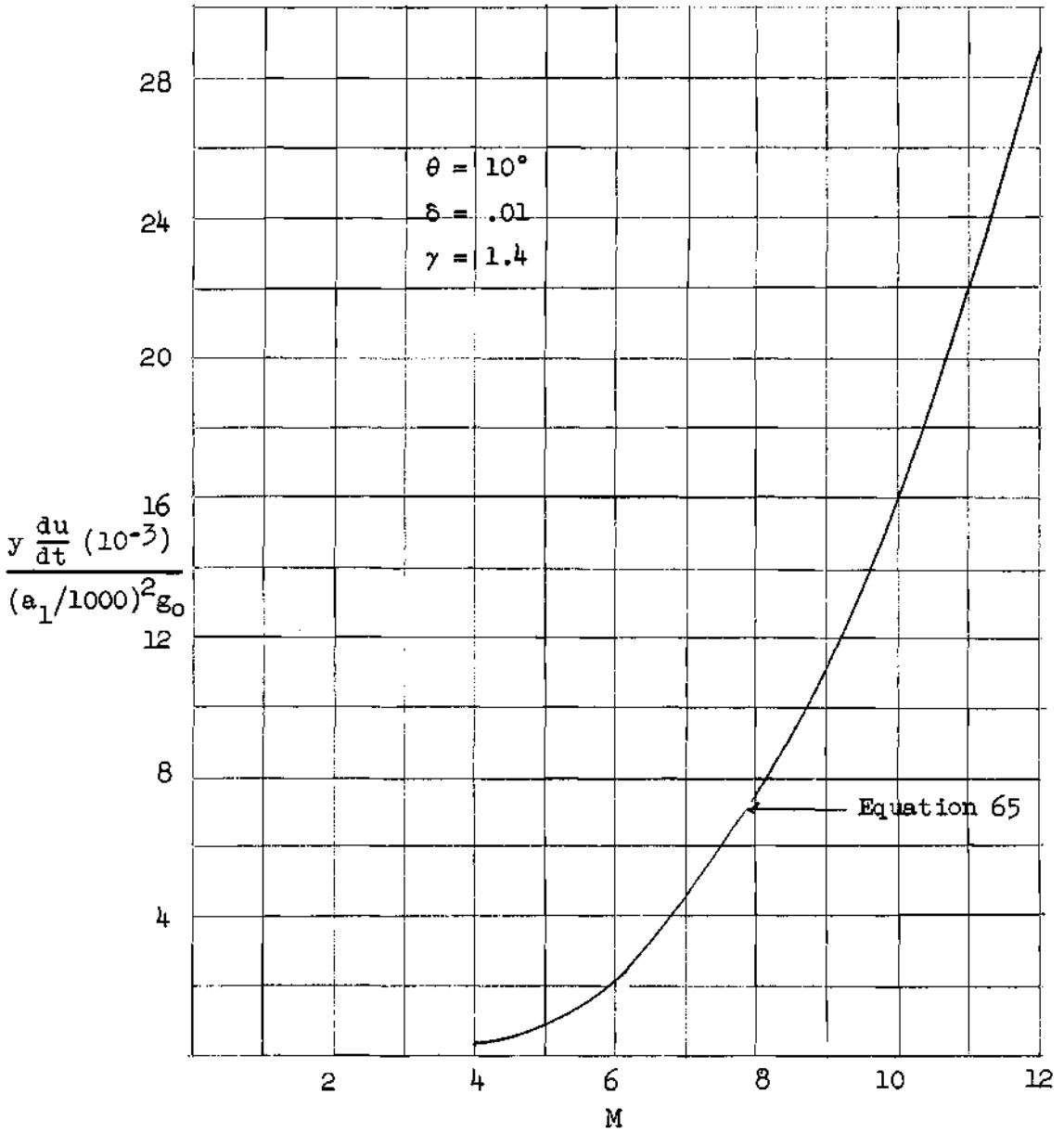

Figure 14. Illustration of Steady State Nature of Problem.

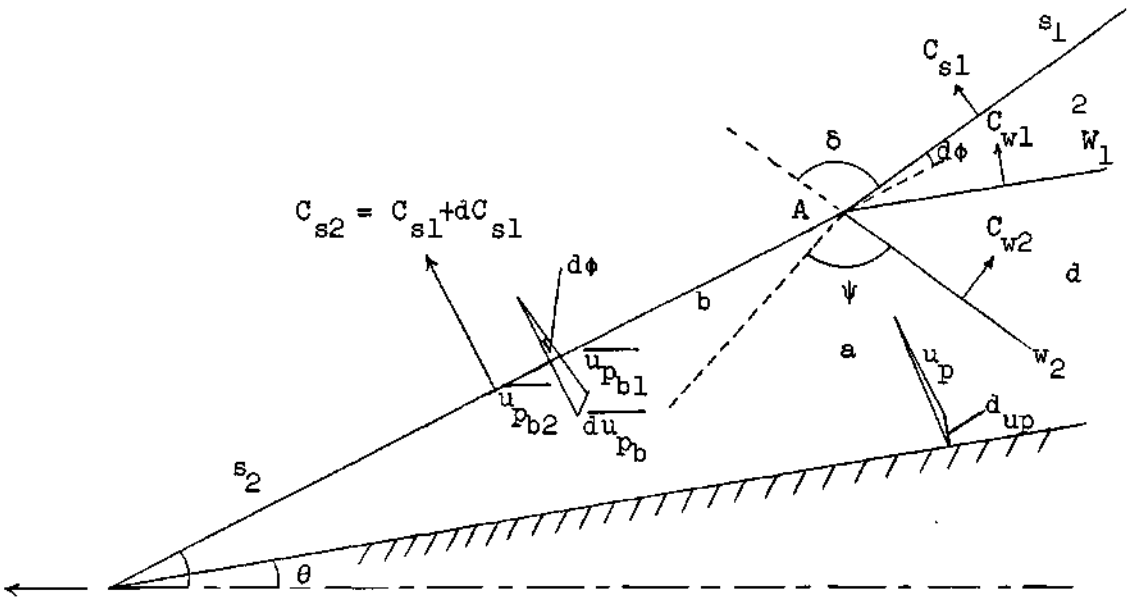

a) Conditions at Shock wave

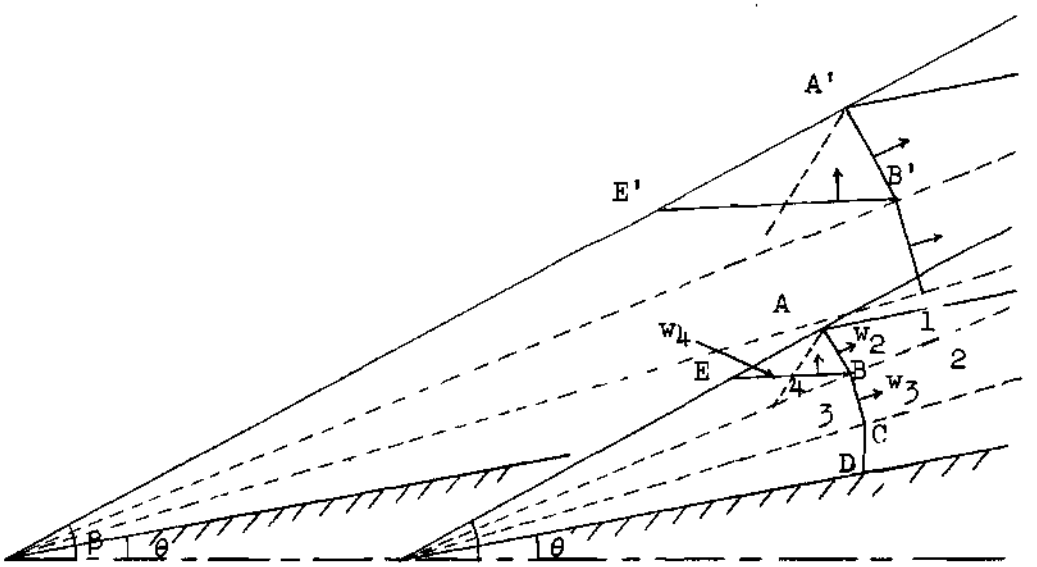

b) Wave network

Figure 15. Illustration of Supersonic Case.

BIBLIOGRAPHY

1. Force, C. T., "Sandia's D-A and V-A Sounding Rockets," Astronautics, Vol. 6, Number 7, 1961, pages 38-64.

2. Gardner, C. S., Ludloff, H. F., and Reiche, F., "Drag of an Airfoil in Accelerated Supersonic Flight," Journal of Applied Physics Vol. 19, December 1948, pages 1179-1180.

3. Frankl, F. I., Effect of the Acceleration of Elongated Bodies of Revolution Upon the Resistance in a Compressible Flow, United States National Advisory Committee for Aeronautics, Technical Memorandum 1230, May 1949.

4. Cole, J. D., "Acceleration of Slender Bodies of Revolution Through Sonic Velocity," Journal of Applied Physics, Vol. 26, September 1952, pages 301-317.

5. Gardner, C. S., and Ludloff, H. F., "Influence of Acceleration on Aerodynamic Characteristics of Thin Airfoils in Supersonic and Transonic Flight," Journal of the Aeronautical Sciences, Vol. 17, 1 January 1950, pages 47-59.

6. Lighthill, M. J., "Oscillating Airfoils at High Mach Numbers," Journal of the Aeronautical Sciences, Vol. 20, June 1953, pages 402-406.

7. Foa, J. V., Elements of Flight Propulsion, John Wiley and Sons, Inc., New York, 1960, pages 90-161.

8. Liepmann, H. W., and Roshko, A., Elements of Gasdynamics, John Wiley and Sons, Inc., New York, 1957, page 64.